cmgh
CELLULAR AND MOLECULAR GASTROENTEROLOGY AND HEPATOLOGY

ORIGINAL RESEARCH

Additive Effect of CD73 Inhibitor in Colorectal Cancer Treatment With CDK4/6 Inhibitor Through Regulation of PD-L1

Ji-Yoon Noh,[1] In Pyo Lee,[2,3] Na Rae Han,[2,3] Miok Kim,[2,3] Yong Ki Min,[2,3] Sang-Yeop Lee,[4] Sung Ho Yun,[5] Seung Il Kim,[4] Tamina Park,[6] Hyunmin Chung,[1,7] Daeui Park,[6,*] and Chang Hoon Lee[2,3,*]

[1]Aging convergence research center, Korea Research Institute of Bioscience and Biotechnology (KRIBB), Daejeon, Republic of Korea; [2]R&D Center, SCBIO Co, Ltd, Daejeon, Republic of Korea; [3]Therapeutics & Biotechnology Division, Drug Discovery Platform Research Center, Korea Research Institute of Chemical Technology (KRICT), Daejeon, Republic of Korea; [4]Research Center for Bioconvergence Analysis, Korea Basic Science Institute, Ochang, Republic of Korea; [5]Center for Research Equipment, Korea Basic Science Institute, Ochang, Republic of Korea; [6]Department of Predictive Toxicology, Korea Institute of Toxicology (KIT), Daejeon, Korea; and [7]College of Pharmacy, Chungnam National University, Daejeon, Republic of Korea

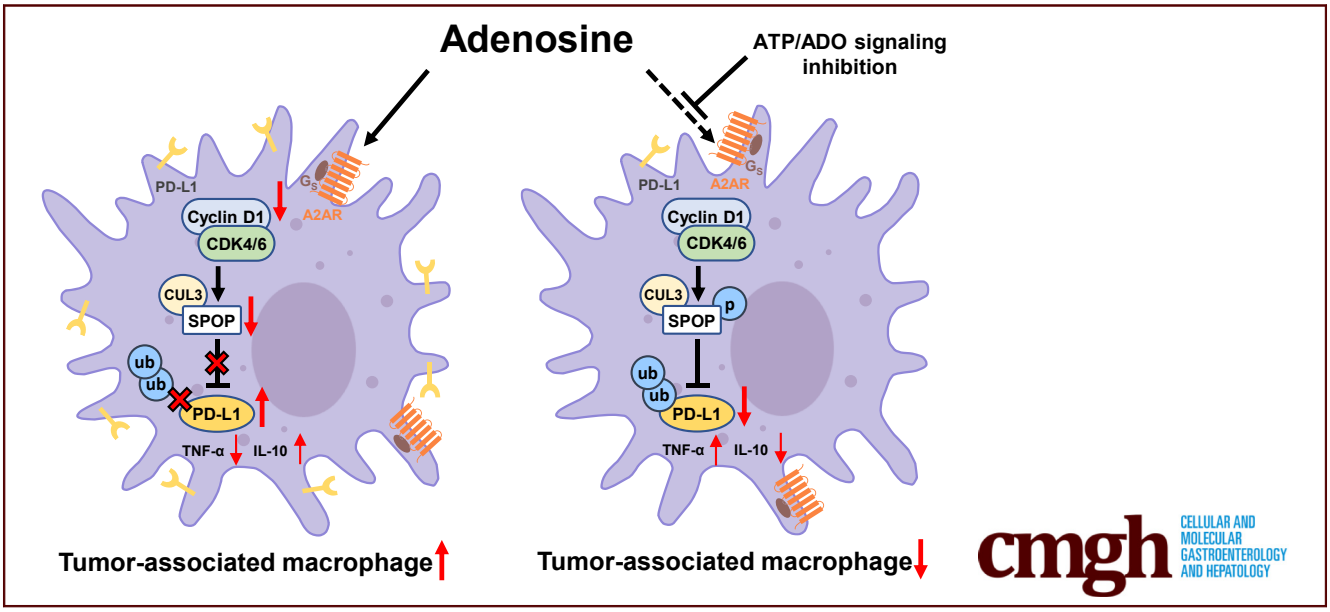

SUMMARY

Extracellular adenosine upregulates programmed death-ligand 1 (PD-L1) in tumor-associated macrophages. A selective CD73 inhibitor suppresses PD-L1 expression, and represents anti-tumor effect in colorectal cancer (CRC) models. The combination of AB680 and palbociclib may be advantageous for treatment of CRC.

BACKGROUND & AIMS: Although cancer immunotherapies are effective for advanced-stage cancers, there are no clinically approved immunotherapies for colon cancers (CRCs). Therefore, there is a high demand for the development of novel therapies. Extracellular adenosine-mediated signaling is considered a promising target for advanced-stage cancers that are nonresponsive to programmed death 1 (PD-1)-/programmed death-ligand 1 (PD-L1)-targeted immunotherapies. In this study, we aimed to elucidate novel tumorigenic mechanisms of extracellular adenosine.

METHODS: To investigate the effects of extracellular adenosine on tumor-associated macrophages, peripheral blood-derived human macrophages were treated with adenosine and analyzed using flow cytometry and Western blot. Changes in adenosine-treated macrophages were further assessed using multi-omics analysis, including total RNA sequencing and proteomics. Colon cancer mouse models were used to measure the therapeutic efficacy of AB680 and palbociclib. We also used tissue microarrays of patients with CRC, to evaluate their clinical relevance.

RESULTS: Extracellular adenosine-mediated reduction of cyclin D1 (CCND1) was found to be critical for the regulation of immune checkpoint molecules and PD-L1 levels in human macrophages, indicating that post-translational modification of PD-L1 is affected by adenosine. A potent CD73 selective inhibitor, AB680, reversed the effects of adenosine on CCND1 and PD-L1. This result strongly suggests that AB680 is a combinatory therapeutic option to overcome the undesired side effects of the cyclin-dependent kinase 4/6 inhibitor, palbociclib, which increases PD-L1 expression in tumors. Because palbociclib is

undergoing clinical trials for metastatic CRC in combination with cetuximab (clinical trial number: NCT03446157), we validated that the combination of AB680 and palbociclib significantly improved anti-tumor efficacy in CRC animal models, thereby highlighting it as a novel immunotherapeutic strategy. We further assessed whether the level of CCND1 in tumor-associated macrophages was indeed reduced in tumor sections obtained from patients with CRC, for evaluating the clinical relevance of this strategy.

CONCLUSIONS: In this study, we demonstrated that a novel combination therapy of AB680 and palbociclib may be advantageous for the treatment of CRC. *(Cell Mol Gastroenterol Hepatol 2022;14:769–788; https://doi.org/10.1016/j.jcmgh.2022.07.005)*

Keywords: CD73 Ecto-enzyme; Colorectal Cancer; Extracellular Adenosine; Programmed Death-Ligand 1.

Cancer immunotherapy has demonstrated incomparable therapeutic efficacy in several cancers, including melanoma, lung cancer, and lymphoma, and has thus become a cornerstone of advanced-stage cancer therapy.[1] Nevertheless, cancer immunotherapy drugs, such as pembrolizumab, nivolumab, and atezolizumab, which target programmed cell death protein 1 (PD-1) and programmed death-ligand 1 (PD-L1), have shown limited responses in colorectal cancer (CRC).[2-5] Moreover, CRC is a prominent disease with high rates of morbidity and mortality,[6] and is characterized by complex immune responses and close interactions between cancer cells and intratumoral immune cells.[2,7] Therefore, there is an urgent need for the development of novel immunotherapies for CRCs.

Tumor-associated macrophages (TAMs) are critical cellular components of the mucosal immune system in CRC, which serve as a bridge between intestinal tumor-promoting metabolites and the onset and progression of CRC through inflammatory pathways.[8,9] TAMs can influence resistance to anti-cancer treatments, such as chemotherapy and anti-PD-1/PD-L1 therapy, and abundance of TAMs is associated with poor prognosis in various tumors.[10,11] TAMs express PD-L1, and PD-L1-expressing TAM levels in tumors may be used as predictive markers for the efficacy of anti-PD-1/PD-L1 therapies.[12] TAMs also increase other immunosuppressive molecules such as CD39 (also known as ectonucleoside triphosphate diphosphohydrolase 1, ENTPD1), CD73 (also known as ecto-5'-nucleotidase, NT5E), arginases, and indoleamine 2,3-dioxygenases.[12-14] Ectoenzymes CD39 and CD73 generate adenosine extracellularly from adenosine triphosphate (ATP) and adenosine monophosphate (AMP), respectively.[15-17] Recently, extracellular adenosine signaling has emerged as a key metabolic pathway that regulates tumor immunity and serves as a tumorigenic factor in CRC.[16,18-20] Adenosine-associated molecules in the tumor microenvironment (TME), such as adenosine receptors and the ectoenzymes CD73 and CD39, are thought to be novel immune checkpoints that play key roles in tumor growth, metastasis,[21] and TAM upregulation.[14] A potent and selective CD73 inhibitor, AB680, and selective adenosine A2Areceptor antagonist, CPI-444, are currently undergoing phase I clinical trials.[22-24] Notably, a recent phase I clinical trial revealed higher efficacy of the combination of CPI-444 and a PD-L1 inhibitor, atezolizumab, in the treatment of renal cell cancer,[24] suggesting that blockade of the adenosine signaling pathway could be beneficial for immunotherapy-resistant tumors. In addition, CD73 inhibition has shown potential therapeutic efficacy in CRC, upon single-cell RNA sequencing (scRNA-seq) analysis of mouse models in our previous study.[25]

Although TAMs are known to express PD-L1, the exact mechanism underlying the simultaneous upregulation of PD-L1 in TAMs has not been elucidated. Importantly, it has been reported that suppression of cyclin D1 (CCND1) may be involved in PD-L1 protein accumulation, via regulation of protein ubiquitination.[26] Several studies have demonstrated that CD73 expression is elevated in metastatic carcinomas or tumors in the A2A adenosine receptor-deficient mouse model.[27,28] The adenosine receptor-mediated accumulation of intracellular cyclic AMP (cAMP) can lead to TAM development and an immunosuppressive TME.[29] In this study, we aimed to elucidate the novel tumorigenic mechanisms of extracellular adenosine in CRC via the upregulation of PD-L1 in TAMs. We demonstrated that a potent and selective CD73 inhibitor, AB680, could limit extracellular adenosine signaling-mediated increase in PD-L1 expression. Furthermore, a clinically approved cyclin-dependent kinase 4/6 (CDK4/6) inhibitor, palbociclib, showed synergistic effects with AB680 in vivo, suggesting novel combinatorial immunotherapies for treating CRC. We believe that AB680 could compensate for the shortcomings of a large portion of anticancer therapies that trigger increased expression of PD-L1, which is a major obstacle for cancer treatment.[30,31]

Results

Extracellular ATP/Adenosine Signaling Increases PD-L1 Expression in Macrophages

To examine the effects of extracellular adenosine on the expression of immune checkpoints or immune-related molecules in macrophages, human peripheral blood (PB) monocyte-derived $CD68^{+}$ macrophages were analyzed for 56

*Authors share co-corresponding authorship.

Abbreviations used in this paper: **AMP, adenosine monophosphate; AOM, azoxymethane; ATP, adenosine triphosphate; cAMP, cyclic AMP; CCND1, cyclin D1; CD39, ectonucleoside triphosphate diphosphohydrolase-1; CD73, ecto-5'-nucleotidase; CDK 4/6, cyclin-dependent kinase 4/6; CRC, colorectal cancer; CUL3/4B, Cullin-3/4B; DEG, differentially expressed gene; DEP, differentially expressed protein; DSS, dextran sulfate sodium; ELISA, enzyme-linked immunosorbent assay; FBS, fetal bovine serum; GO, Gene Ontology; IHC, immunohistochemical; IL, interleukin; IP, immunoprecipitation; LC-MS/MS, liquid chromatography-tandem mass spectrometry; M-CSF, macrophage colony-stimulating factor; PB, peripheral blood; PD-1, programmed death 1; PD-L1, programmed death-ligand 1; RNA-seq, RNA sequencing; scRNA-seq, single-cell RNA sequencing; shRNA, short hairpin RNA; SPOP, speckle-type POZ protein; TAM, tumor-associated macrophage; TCGA, The Cancer Genome Atlas; 3D, 3-dimensional; TNF, tumor necrosis factor; TME, tumor microenvironment.**

Most current article

2352-345X
https://doi.org/10.1016/j.jcmgh.2022.07.005

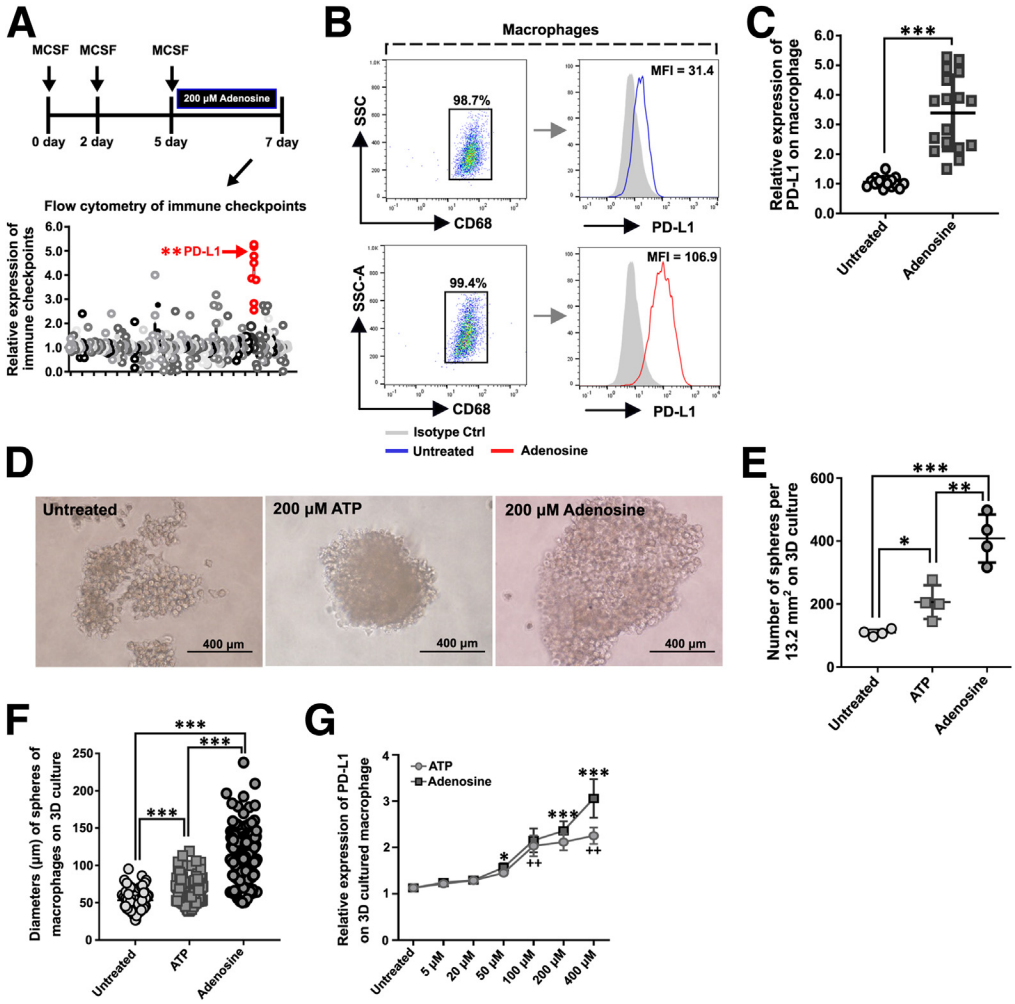

Figure 1. Effects of extracellular adenosine on CCND1 levels and PD-L1 expression in human macrophages. (*A*) Experimental scheme for human macrophage differentiation from PB and adenosine treatment (*upper panel*). Flow cytometric analysis for 56 immune-related molecules (n = 7). Relative amounts of immune-related molecules on macrophages treated with or without 200 μM adenosine for 48 hours, as analyzed shown through flow cytometry. (*B*) PD-L1 expression on $CD68^+$ human macrophages after treatment with 200 μM adenosine for 48 hours. Mean fluorescence intensity (MFI) of PD-L1 relative to an isotype control (n = 11). (*C*) Relative amount of PD-L1 protein on macrophages treated with or without 200 μM adenosine for 48 h (n = 18) (*D*) Representative images of 3D-cultured macrophages treated with 200 μM ATP or 200 μM adenosine for 48 hours; the results are from 4 independent experiments. Scale bars have been presented. Pooled data indicating ATP- or adenosine-induced sphere-forming capability in macrophages, as measured using (*E*) sphere number and (*F*) sphere diameter (the longest sphere diameters). Experiments were performed in triplicate. (*G*) Dose-dependent increase in PD-L1 levels following ATP and adenosine treatment in the 3D-culture system (n = 5). Data have been presented as mean ± standard error of the mean. ns, not significant. $^*P < .05$, $^{**}P < .01$, $^{***}P < .001$, and $^{++}P < .01$ (Student *t* test).

different immune-related molecules using flow cytometry (Figure 1, *A*). Among the 56 immune-related molecules (Table 1), a significant increase was observed in the expression of the tumorigenic protein PD-L1 (Figure 1, *A*). We further confirmed the results of flow cytometry and Western blot (Figure 1, *B*–*C*). To determine the actual ATP-to-adenosine conversion in the TME, we evaluated the effects of extracellular ATP on human macrophages in a 3-dimensional (3D) environment using agarose-based 3D cultures. In 3D cultures, we observed that the macrophages aggregated to form 3D spheres (Figure 1, *D*). The number and diameter of macrophage spheres significantly increased following exposure to extracellular ATP and adenosine (Figure 1, *E*–*F*). PD-L1 expression levels were increased in a dose-dependent manner by both ATP and adenosine in the 3D culture systems, thereby highlighting that ATP was indeed converted to adenosine in the 3D macrophage sphere environment (Figure 1, *G*).

Extracellular Adenosine Increases PD-L1 Through Transcriptional-downregulation of Cyclin D1 in Macrophages

To understand the transcriptional changes induced in macrophages by extracellular adenosine, we performed RNA sequencing (RNA-seq) of untreated macrophages and those treated with 200 μM adenosine. Differentially expressed genes

Table 1. List of Immune-related Molecules of Human Macrophages Analyzed by Flow Cytometry

Target protein	Mean ± SEM	Target protein	Mean ± SEM
CD70	2.51 ± 1.84	CD39	1.01 ± 0.09
GITRL	1.13 ± 0.25	CD163	1.25 ± 1.48
CD40L	0.93 ± 0.29	CD206	1.15 ± 0.23
CD86	0.96 ± 0.15	CTLA-4	0.93 ± 0.20
MHC I	1.74 ± 1.82	CX3CR1	2.27 ± 2.46
IDO-1	1.36 ± 1.95	HLA-A, B, C	1.30 ± 0.42
Itg avb3	1.02 ± 0.25	HLA-DR	1.03 ± 0.17
Lag3	1.31 ± 0.68	PD-L1	2.92 ± 0.41
Galectin9	1.01 ± 0.11	CD155	0.93 ± 0.11
CD80	1.22 ± 0.17	CD38	1.26 ± 0.83
HVEM	1.04 ± 0.07	CD69	1.04 ± 0.07
4-1BB	1.11 ± 0.11	CD62L	1.05 ± 0.20
CD56	0.98 ± 0.61	CD161	1.02 ± 0.09
CD34	1.04 ± 0.09	CD40	1.07 ± 0.58
ICOS-L	0.92 ± 0.27	DDR1	1.02 ± 0.06
CD73	1.08 ± 0.07	CD44	1.16 ± 0.30
NKp46	1.05 ± 0.05	CCR6	1.03 ± 0.12
NKG2D	0.97 ± 0.89	CXCR6	1.06 ± 0.08
NKp80	1.46 ± 1.78	CCR2	1.05 ± 0.09
LAMP-1	0.94 ± 0.11	CCR1	0.90 ± 0.14
CD47	1.03 ± 0.20	I-CAM	1.03 ± 0.59
DR5	4.39 ± 3.57	CCR5	0.95 ± 0.08
DcR1	0.86 ± 0.51	MHC II	0.84 ± 0.31
CD94	0.95 ± 0.27	CCL2	1.10 ± 0.52
CD158	1.06 ± 0.16	CCR7	1.07 ± 0.06
DR4	1.05 ± 0.13	HLA-E	1.22 ± 0.17
Tyro3	1.08 ± 0.12	MICA&B	1.04 ± 0.33
CD58	0.94 ± 0.29	PD-L2	1.14 ± 0.19

SEM, Standard error of the mean.

(DEGs) were found to be involved in cell cycle, cell division, cell cycle phase transition, and DNA repair (Figure 2, *A*). The expression of one of the most notable cell cycle-related genes (DEG number 50), *CCND1*, which is a gene encoding cyclin D1, was significantly lower in extracellular adenosine-treated macrophages than that in untreated macrophages (Figure 2, *B*). To verify our findings, we assessed the differences in the expression levels of 3 cyclin D family genes using quantitative real-time polymerase chain reaction and confirmed that only *CCND1* levels were significantly reduced upon adenosine treatment (Figure 2, *C*). The protein level of CCND1 also decreased, whereas the levels of CDK4 remained unchanged (Figure 2, *D–E*). To examine the relationship between alterations in the expression of *CCND1* and PD-L1 protein in human macrophages, we introduced a short hairpin RNA (shRNA) against *CCND1*, which resulted in a significant increase in PD-L1 protein levels (Figure 2, *F–G*). Adenosine slightly enhanced PD-L1 levels in the presence of shRNAs, indicating that reduction of *CCND1* is the main mechanism of action in PD-L1 elevation (Figure 2, *G*). Fifty-four DEGs were found to be associated with CCND1, indicating that adenosine regulates the CCND1 signaling pathway in human macrophages (Figure 3, *A*). Notably, Gene Ontology (GO) enrichment analysis revealed that cell cycle G1/S phase transition (GO:0044843) and negative regulation of interleukin (IL)-12 production (GO:0032695) were primarily affected by extracellular adenosine, suggesting that adenosine could induce immunosuppressive effects on macrophages (Figure 3, *B*). To determine whether adenosine altered the immune function of macrophages, we analyzed 33 cytokine-related DEGs. Immune-suppressive genes, such as *IL-10*, *LILRA5*, *LILRB1*, and *THBS1* were also enriched in adenosine-treated macrophages (Figure 4).

Extracellular Adenosine Leads to Critical Changes for Protein Ubiquitination-related Proteins Binding to PD-L1 Protein in Macrophages

To understand the effect of extracellular adenosine on the post-translational regulation of PD-L1, we compared extracellular adenosine-treated macrophages with untreated macrophages using liquid chromatography-tandem

mass spectrometry (LC-MS/MS) followed by immunoprecipitation (IP) with PD-L1, to identify the distinct proteins interacting with PD-L1. Such an analysis resulted in the identification of proteins that interacted with PD-L1, of which 359 differentially expressed proteins (DEPs) were significantly upregulated proteins, whereas 468 DEPs were

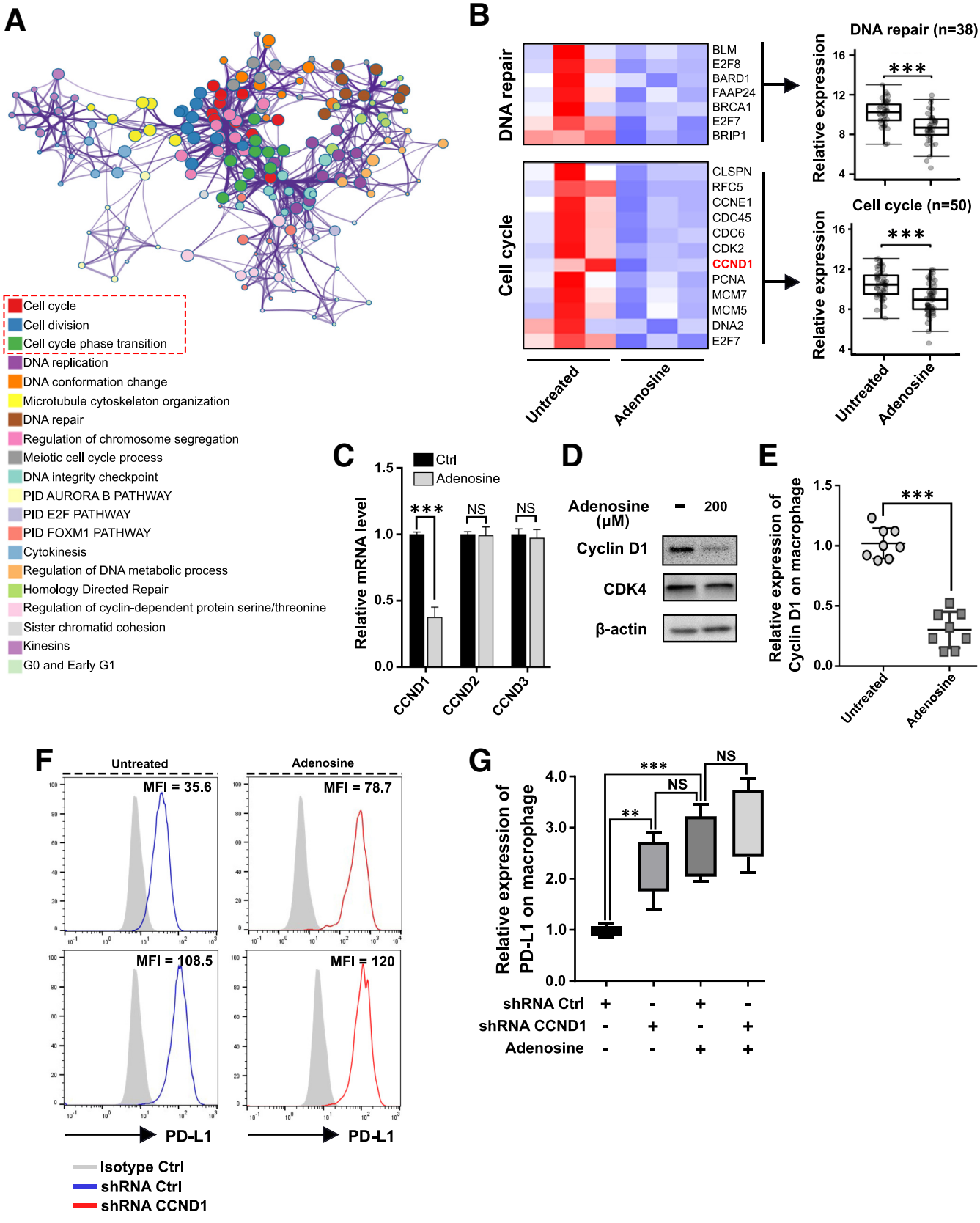

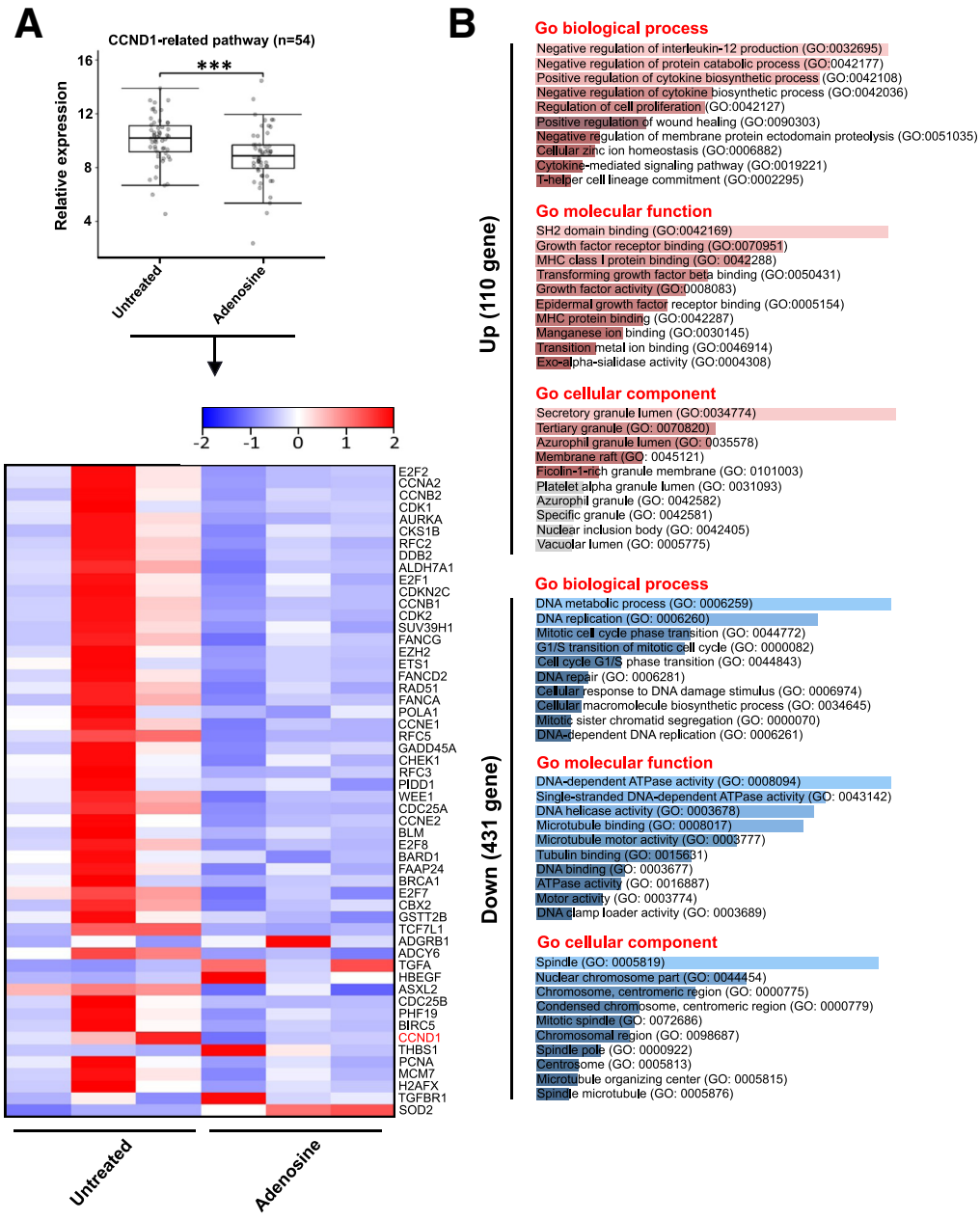

Figure 3. DEGs of *CCND1*-related pathway from extracellular adenosine treated macrophages. (*A*) Comparative RNA-seq analysis of untreated and adenosine (200 μM)-treated human macrophages. Genes most significantly influenced by adenosine treatment: CCND1-related (54 genes). (*B*) Results of the GO enrichment analysis of total DEGs from extracellular adenosine-treated human macrophages compared with untreated macrophages. Data have been presented as mean ± standard error of the mean. ***$P < .001$ (Student *t* test).

significantly downregulated (Figure 5, *A*). The majority of PD-L1-interacting proteins in adenosine-treated macrophages were related to ubiquitin-protein transferase inhibitor activity (GO term: 0055105), mitotic cell cycle phase transition (GO term: 0044772), and regulation of protein ubiquitination (GO term: 0051444) (Figure 5, *B*).

Figure 2. (***See previous page***). **Adenosine-induced decrease in CCND1 levels drives PD-L1 protein upregulation.** (*A*) Comparative RNA-seq analysis of untreated and adenosine (200 μM)-treated human macrophages. In the network, each node represents a GO biological pathway, and the edges indicate the relationships among biological pathways, based on kappa values. (*B*) Genes most significantly influenced by adenosine treatment: cell cycle-related (50 genes) and DNA damage repair-related (38 genes). Cyclin D1 (*CCND1*) was selectively decreased upon adenosine treatment, at the mRNA (n = 4) (*C*) and protein levels (n = 7) (*D, E*). (*F*) Representative histogram of 5 independent experiments and (*G*) quantitative measurements of PD-L1 expression following treatment with anti-*CCND1* shRNA or negative control shRNA in the presence or absence of adenosine (200 μM) treatment, as analyzed using fluorescence-activated cell sorting analysis. Data have been presented as mean ± standard error of the mean. ns, not significant. ***$P < .001$ (Student *t* test).

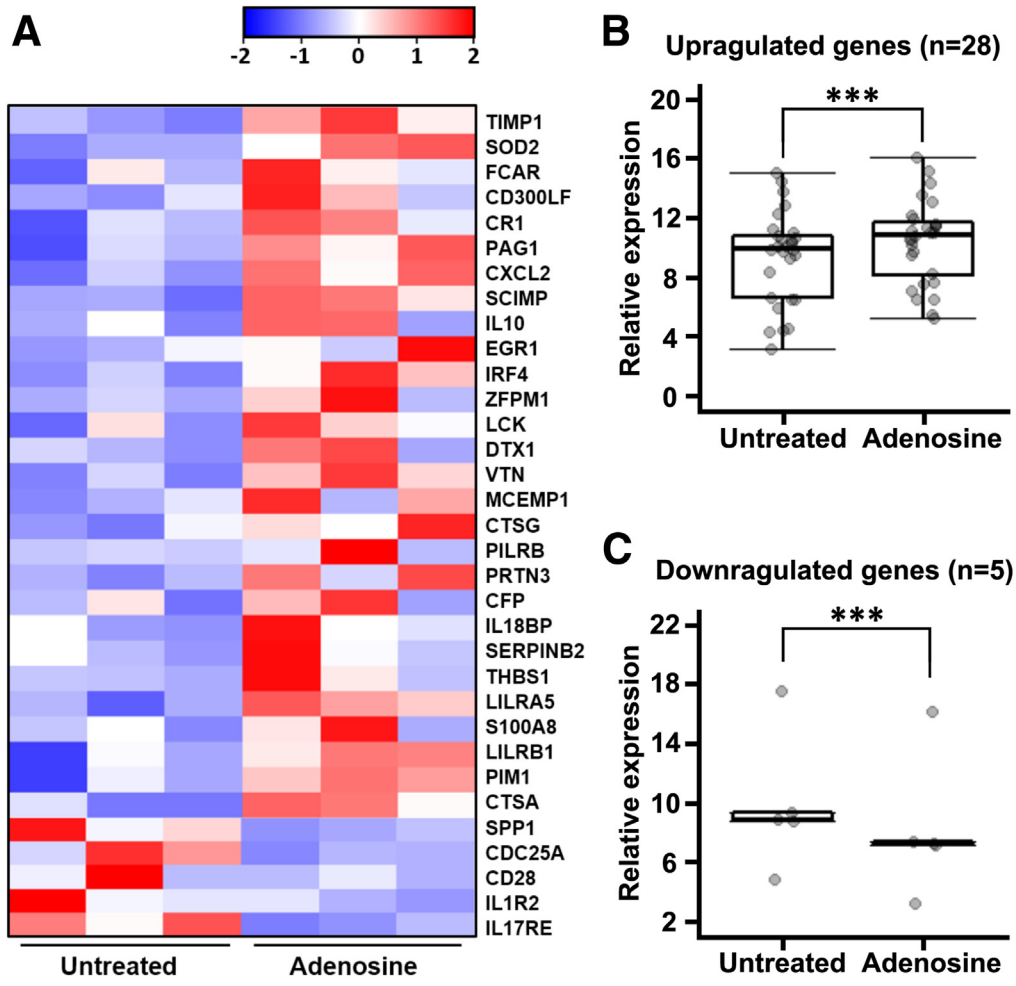

Figure 4. Analysis of altered cytokine-related gene expressions. (*A*) Heat map of cytokine and immune related DEGs from extracellular adenosine-treated human macrophages compared with untreated macrophages. (*B*–*C*) Upregulated genes and downregulated genes in adenosine treated macrophages were respectively compared to untreated macrophages. Data have been presented as mean ± standard error of the mean. ***$P < .001$ (paired *t* test).

Using enrichment analysis, cell cycle- and ubiquitination-related terms were identified to be the most enriched in biological processes (Figure 5, *B*). We also performed functional network analysis of 65 DEPs associated with the GO terms of cell cycle and ubiquitination, resulting in the identification of cullin-3 (CUL3) and cullin-4B (CUL4B) (Figure 5, *C*). To confirm the post-regulation of PD-L1 expression, we treated human macrophages with or without the proteasome inhibitor MG132 (Figure 5, *D*). Notably, PD-L1 expression in human macrophages was significantly upregulated after treatment with the proteasome inhibitor, MG132 (Figure 5, *D*–*E*). Thus, we hypothesized that post-translational regulation is a critical mechanism for increasing PD-L1 expression in macrophages exposed to extracellular adenosine.

CUL3, CUL4B, and Speckle-type POZ Protein (SPOP) Act as Post-translational Regulators of PD-L1 in Human Macrophages

Notably, CUL3 and CUL4B were significantly enriched among PD-L1-interacting DEPs, upon adenosine treatment (Figure 5, *C*). These proteins are components of cullin-RING E3 ubiquitin ligase complexes.[32,33] In addition, CUL3 has been suggested to mediate PD-L1 ubiquitination, followed by protein degradation in cancer cells.[27] Thus, we confirmed the interaction between PD-L1 and CUL3 using co-immunoprecipitation (co-IP) analysis (Figure 6, *A*). To verify the role of CUL3 in human macrophages, we knocked down CUL3 in cells and measured PD-L1 levels using flow cytometry. A significant increase was observed in PD-L1 levels in human macrophages (Figure 6, *B*–*C*). Interestingly, CUL4B had the same effects on the regulation of PD-L1, suggesting that CUL3- and CUL4B-mediated protein degradation may play a critical role in PD-L1 expression in human macrophages (Figure 6, *D*–*F*). To confirm this, we treated macrophages with MLN4924, a NEDD8 ubiquitination pathway inhibitor,[34] and observed upregulation of PD-L1 expression (Figure 6, *G*–*H*). In contrast, treatment with bafilomycin A1, an autophagy inhibitor, did not significantly affect PD-L1 expression (Figure 6, *G*–*H*).

SPOP is an adaptor protein for cullin-RING E3 ubiquitin ligases, which have been reported to be modulated by CCND1 and CDK4 during the cell cycle.[26] Therefore, we tested whether SPOP is affected by adenosine treatment, and found that SPOP expression in human macrophages was indeed reduced by extracellular adenosine (Figure 6, *I*–*J*). SPOP bound to PD-L1 (Figure 6, *K*), in agreement with a previous report.[26] To confirm the involvement of SPOP in

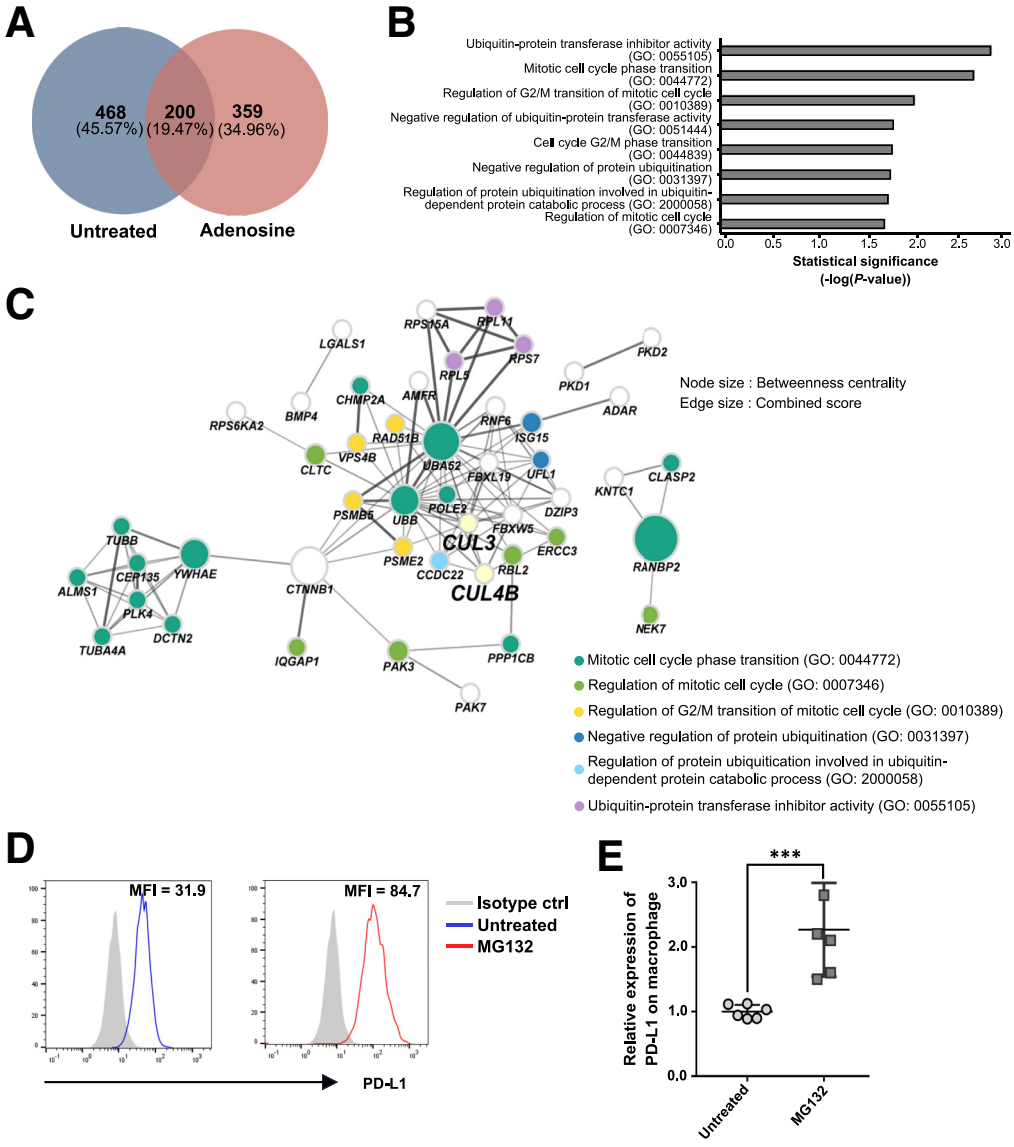

Figure 5. Proteomics analysis revealed that PD-L1 binds to multiple post-translational regulators in macrophages stimulated with extracellular adenosine. (*A*) Venn diagram of the numbers of PD-L1-interacting proteins, as identified using LC-MS/MS analysis, in adenosine (200 μM)-treated and untreated human macrophages. (*B*) Results of the GO enrichment analysis of DEPs. (*C*) Functional network analysis of 65 DEPs associated with the GO terms of cell cycle and ubiquitination, using IP tools. (*D*) Representative histogram of 5 independent experiments; and (*E*) quantification of PD-L1 expression after treatment with 10 μM MG132 for 48 hours. Data have been presented as mean ± standard error of the mean. ***$P < .001$ (Student *t* test).

the post-translational regulation of PD-L1, we knocked down *SPOP* using an shRNA and found that SPOP levels were crucial in regulating PD-L1 expression. SPOP knockdown upregulated PD-L1 expression in macrophages (Figure 6, *L*–*M*), suggesting that cullin-mediated PD-L1 protein regulation may occur in macrophages, similar to previous findings.[26]

The Potent and Selective CD73 Inhibitor, AB680, Improved the Therapeutic Efficacy of a CDK4/6 Inhibitor, Palbociclib, Suggesting a Novel Combinatory Immunotherapeutic Strategy for CRC

To verify our findings, we treated human macrophages with a selective CD73 inhibitor, AB680, and an adenosine A2A receptor antagonist, CPI-444 (also known as ciforadenant), in the presence and absence of ATP (Figure 7, *A*). PB-derived human macrophages expressed CD73 on their surface, indicating their ability to convert extracellular ATP to adenosine (Figure 7, *A*). Both AB680 and CPI-444 treatments significantly reduced the amount of PD-L1 protein on the surface of ATP-exposed macrophages, as compared with that in the ATP-alone treatment group (Figure 7, *A*–*B*). To determine whether these effects are mediated by adenosine receptors in human macrophages, we measured the levels of intracellular cAMP. Treatment with ATP and AB680 suppressed ATP-derived cAMP levels, suggesting the involvement of the adenosine receptor (Figure 7, *C*). In macrophages, upregulation of cAMP could lead to immunosuppressive effects,[29] and both the suppression of tumor necrosis factor (TNF)-α and increase in IL-10 were reversed upon AB680 or CPI-444 treatment (Figure 7, *D*). These results strongly suggest that AB680 may have anti-tumor efficacy via the regulation of cAMP, the immunosuppressive functions of which include an increase in IL-10 and PD-L1 expression. Thus, it is an attractive therapeutic option to use AB680 as a combination drug for PD-L1 suppression. In

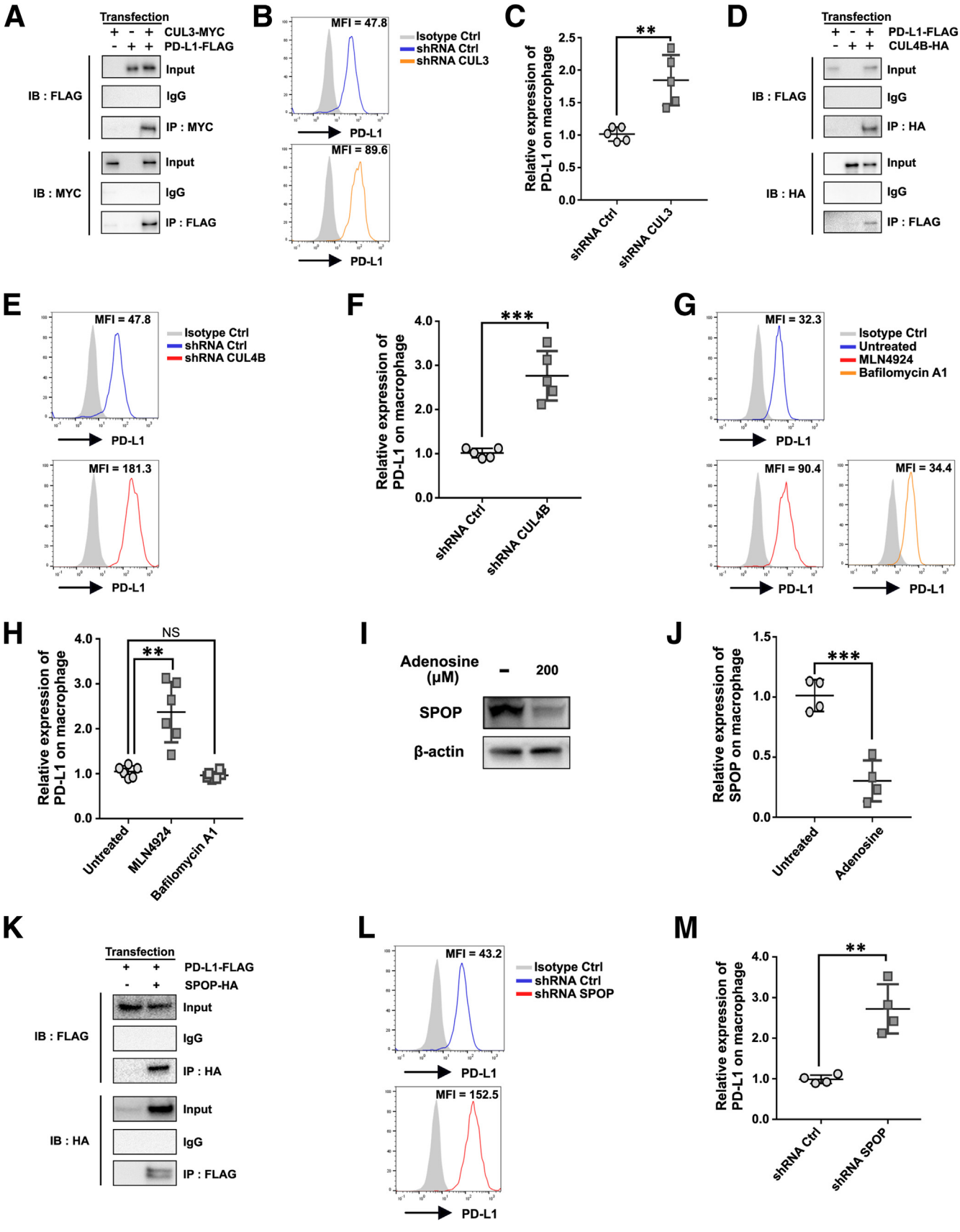
A
Transfection
+ - + CUL3-MYC
- + + PD-L1-FLAG
IB : FLAG
Input
IgG
IP : MYC
IB : MYC
Input
IgG
IP : FLAG
B
MFI = 47.8
Isotype Ctrl
shRNA Ctrl
shRNA CUL3
PD-L1
MFI = 89.6
PD-L1
C
Relative expression of PD-L1 on macrophage
**
shRNA Ctrl
shRNA CUL3
D
Transfection
+ - + PD-L1-FLAG
- + + CUL4B-HA
IB : FLAG
Input
IgG
IP : HA
IB : HA
Input
IgG
IP : FLAG
E
MFI = 47.8
Isotype Ctrl
shRNA Ctrl
shRNA CUL4B
PD-L1
MFI = 181.3
PD-L1
F
Relative expression of PD-L1 on macrophage
***
shRNA Ctrl
shRNA CUL4B
G
MFI = 32.3
Isotype Ctrl
Untreated
MLN4924
Bafilomycin A1
PD-L1
MFI = 90.4
PD-L1
MFI = 34.4
PD-L1
H
Relative expression of PD-L1 on macrophage
NS
**
Untreated
MLN4924
Bafilomycin A1
I
Adenosine (μM)
-
200
SPOP
β-actin
J
Relative expression of SPOP on macrophage
***
Untreated
Adenosine
K
Transfection
+ + PD-L1-FLAG
- + SPOP-HA
IB : FLAG
Input
IgG
IP : HA
IB : HA
Input
IgG
IP : FLAG
L
MFI = 43.2
Isotype Ctrl
shRNA Ctrl
shRNA SPOP
PD-L1
MFI = 152.5
PD-L1
M
Relative expression of PD-L1 on macrophage
**
shRNA Ctrl
shRNA SPOP

this study, we examined the synergistic effect of the CDK4 inhibitor, palbociclib, and AB680 in in vivo models (Figure 7, *E*–*M*). The scheme and representative images of azoxymethane (AOM)-dextran sulfate sodium (DSS) mice, a colitis-associated cancer model, are shown (Figure 7, *E*–*F*). The number of tumors per AOM-DSS mouse was significantly reduced upon treatment with AB680 and palbociclib, which showed an additive effect compared with the monotherapies (Figure 7, *G*). We then isolated TAMs of CRCs from the colitis-associated cancer model, after 21 days of drug administration post the third cycle of DSS treatment, and analyzed the expression of PD-L1. Interestingly, AB680 suppressed PD-L1 on TAMs as opposed to palbociclib, suggesting that AB680 treatment is beneficial in reducing the immunosuppressive effect of TAMs (Figure 7, *H*–*I*). Furthermore, tumor volume was significantly reduced upon treatment with AB680 and palbociclib, and the additive effect was confirmed in the CT26 tumor-bearing mouse model (Figure 7, *J*). The amount of PD-L1 on TAMs was significantly reduced upon treatment with AB680, which is consistent with the result in the colitis-associated cancer model (Figure 7, *K*). Notably, the levels of TNF-α and IL-10 in TAMs were also affected by AB680 administration, suggesting that immunosuppressive TAMs might be functionally reduced by CD73 blockade (Figure 7, *L*–*M*).

Expression of cyclin D1 in Macrophages was Reduced in Tumor Sections Obtained From Patients With CRC as Compared With That in Adjacent Normal Colon Sections, Thus Highlighting its Clinical Relevance

To verify our findings, we performed immunohistochemical (IHC) staining for cyclin D1 and the human macrophage marker CD163 in a human colon tissue array containing 50 specimens of colon adenocarcinoma and matched adjacent normal colon tissues. Macrophages were predominantly localized in the lamina propria but not in the intestinal crypts or mucosa (Figure 8, *A*). Importantly, we quantitatively analyzed the number of cyclin D1-expressing $CD163^+$ macrophages on each slide and found that cyclin D1-expressing macrophages were significantly lower in the lamina propria of colon cancer tissues than in normal colon tissues (Figure 8, *B*). Notably, the mRNA expression of *NT5E* was significantly negatively correlated with *CCND1* in colorectal adenocarcinoma, based on The Cancer Genome Atlas (TCGA) data (Figure 8, *C*). We previously showed that higher *NT5E* expression is associated with a lower survival rate in patients with CRC.[25] Thus, *CCND1* reduction in TAMs may be partially related to CRC progression.

Reclustering Analysis of Myeloid Cells Revealed That Intratumoral $Ccnd1^{low}$ and $Ccnd1^{high}$ Myeloid Cells Showed Distinct Transcriptional Profiles Associated With an Immune-exhausted Phenotype

To understand the changes in cellular composition, lineage, and transcriptional characteristics of myeloid cells from tumors of the CT26 tumor-bearing mouse model, reclustering analysis of the myeloid cells was performed using our previous reported scRNA-seq data of sorted and profiled $CD45^+$ TILs from each tumor of control (n = 3) and AB680-treated (n = 3) mice[25] (data accession number: SUB8983993). After combining all data (n = 6) and reclustering for myeloid cells, we identified 16 myeloid cell subclusters by combining the results of the singleR package and the expression pattern of major myeloid cell lineage markers, as described in our previous report:[25] 5 $Ccnd1^{high}$ TAMs (C3, C7, C10, and C15), 4 $Ccnd1^{low}$ TAMs (C4, C8, C9, and C13), 1 $Ccnd1^{low}$ monocyte (C11), 1 $Ccnd1^{low}$ dendritic cell (C12), and 6 $Ccnd1^{high}$ myeloid-derived suppressor cells (C0, C1, C2, C5, C6, and C14) (Figure 9, *A*). With respect to proportional changes in myeloid clusters, one significant proportional change (C13 cluster) was observed in $Ccnd1^{low}$ TAMs (Figure 9, *B*). Importantly, we found that expression of *Ccnd1* was limited to $Entpd^{low}$ myeloid cells (Figure 9, *C*). The heat map results also showed distinct expression of *Entpd1* and *Ccnd1* (Figure 9*D*). Moreover, we discovered that transcriptional profiles associated with immune-exhausted phenotypes and immune checkpoints, such as *Entpd1* and *Arg2*, were distinctly expressed between intratumoral $Ccnd1^{low}$ and $Ccnd1^{high}$ myeloid cells that included TAMs (Figure 9, *E*–*F*). Based on comparative RNA-seq analysis of $Ccnd1^{low}$ to $Ccnd1^{high}$ myeloid cells, we performed network analysis using GO biological pathways and found that most of the pathways of differences between $Ccnd1^{low}$ and $Ccnd1^{high}$ myeloid cells were immune-related pathways, such as inflammatory response and cytokine signaling (Figure 9, *G*). Taken together, the extracellular

Figure 6. (***See previous page***). **Involvement of CUL3, CUL4B, and SPOP in regulation of PD-L1 protein levels in adenosine-stimulated macrophages.** (*A*) Representative images of co-IP of PD-L1 and CUL3 from 3 independent experiments using 293T cells. (*B*) Representative histogram of 5 independent experiments and (*C*) quantification of PD-L1 expression in human macrophages after knockdown of CUL3 with an shRNA (n = 5). (*D*) Representative images of co-IP of PD-L1 and CUL4B from 3 independent experiments using 293T cells. (*E*) Representative histogram of 5 independent experiments and (*F*) quantification of PD-L1 expression in human macrophages after knockdown of CUL4B with an shRNA (n = 5). (*G*) Representative histogram of 6 independent experiments and (*H*) quantification of PD-L1 expression levels following treatment with 10 μM MLN4924 and 10 μM bafilomycin A1 for 48 hours. (*I*) Representative Western blots; and (*J*) quantification of SPOP levels after adenosine treatment of human macrophages. (*K*) Representative images of co-IP of PD-L1 and SPOP from 3 independent experiments using 293T cells. (*L*) Representative histogram of PD-L1 expression on macrophages after SPOP knockdown. (*M*) Relative PD-L1 expression on macrophages after SPOP knockdown (n = 4). Data have been presented as mean ± standard error of the mean. ns, not significant. $^{**}P < .01$ and $^{***}P < .001$ (Student *t* test).

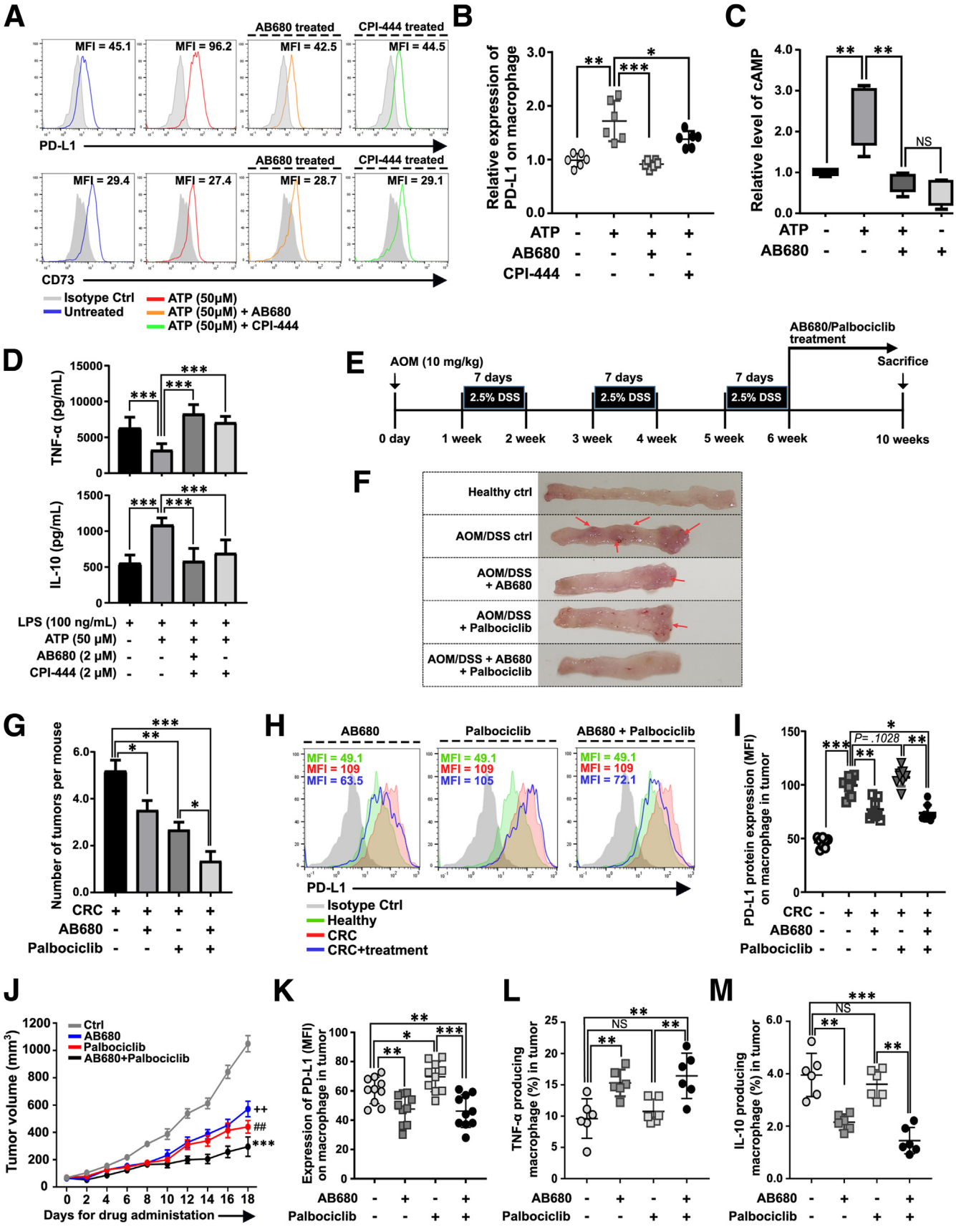
A
AB680 treated
CPI-444 treated
MFI = 45.1
MFI = 96.2
MFI = 42.5
MFI = 44.5
PD-L1
MFI = 29.4
MFI = 27.4
MFI = 28.7
MFI = 29.1
CD73
Isotype Ctrl
Untreated
ATP (50μM)
ATP (50μM) + AB680
ATP (50μM) + CPI-444
B
Relative expression of PD-L1 on macrophage
ATP
AB680
CPI-444
C
Relative level of cAMP
NS
D
TNF-α (pg/mL)
IL-10 (pg/mL)
LPS (100 ng/mL)
ATP (50 μM)
AB680 (2 μM)
CPI-444 (2 μM)
E
AOM (10 mg/kg)
7 days
2.5% DSS
AB680/Palbociclib treatment
Sacrifice
0 day
1 week
2 week
3 week
4 week
5 week
6 week
10 weeks
F
Healthy ctrl
AOM/DSS ctrl
AOM/DSS + AB680
AOM/DSS + Palbociclib
AOM/DSS + AB680 + Palbociclib
G
Number of tumors per mouse
CRC
AB680
Palbociclib
H
AB680
Palbociclib
AB680 + Palbociclib
MFI = 49.1
MFI = 109
MFI = 63.5
MFI = 105
MFI = 72.1
PD-L1
Isotype Ctrl
Healthy
CRC
CRC+treatment
I
PD-L1 protein expression (MFI) on macrophage in tumor
P=.1028
J
Tumor volume (mm3)
Ctrl
AB680
Palbociclib
AB680+Palbociclib
Days for drug administation
K
Expression of PD-L1 (MFI) on macrophage in tumor
L
TNF-α producing macrophage (%) in tumor
M
IL-10 producing macrophage (%) in tumor

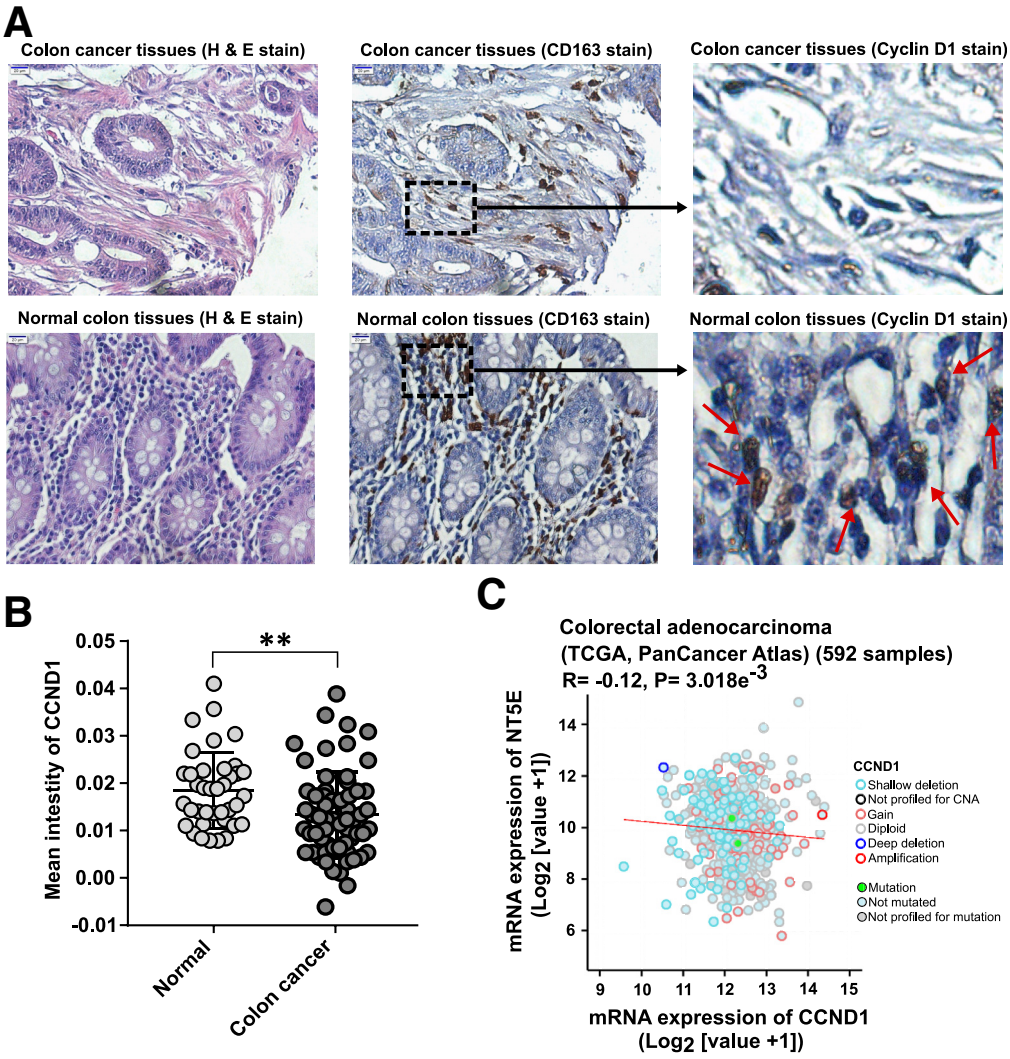

Figure 8. Negative correlation between ecto-enzymes and *CCND1* expression in CRC. (*A*) IHC staining of human normal colon (n = 40) and colon adenocarcinoma (n = 64) specimens in a tissue microarray for CCND1 and CD163 (a macrophage marker). (*B*) Relative intensities of CCND1 staining in the lamina propria of a normal and cancerous colon. $^{**}P < .01$ (unpaired *t* test). (*C*) Correlation analysis of *NT5E* and *CCND1* expression in the TCGA colorectal adenocarcinoma dataset. $^{***}P < .001$ (Student *t* test).

adenosine produced by *Entpd1* and *Nt5e* may enrich *Ccnd1*^{low} myeloid cells, which consist of TAMs and their precursors.

Discussion

An increased concentration of extracellular adenosine is an important determinant of the survival rate of patients

Figure 7. (***See previous page***). **A CD73 inhibitor, AB680, showed a potent synergistic effect to improve therapeutic efficacy of a CDK4 inhibitor, palbociclib for CRC.** (*A*) Representative histograms and (*B*) quantitative measurements of 50 μM ATP-induced PD-L1, CD39, and CD73 expression on macrophages, and the effects of treatment with 2 μM AB680 and CPI-444 (ciforadenant, 2 μM) from 5 independent experiments. (*C*) Relative level of cAMP in human PBMC-derived macrophages treated with or without ATP and AB680. (*D*) Quantitative measurements of TNF-α and IL-10 expression on macrophages treated with or without 2 μM AB680 and CPI-444 in the presence of 50 μM ATP and 100 nM LPS, from 5 independent experiments, using ELISA. (*E*) Outline of the AOM/DSS mouse model of CRC used in this study. (*F*) Representative images of large intestine and (*G*) graphical representation of number of tumors per AOM-DSS mouse administered with AB680 (20 mg/kg) or palbociclib (20 mg/kg) (n = 8 mice per group). (*H*) Representative histograms; and (*I*) quantification for PD-L1 level of TAMs in AOM-DSS mice administered with AB680 (20 mg/kg) or palbociclib (20 mg/kg) (n = 8 mice per group). (*J*) Time courses of tumor volumes in CT26 tumor-bearing mice administered with AB680 (20 mg/kg) or palbociclib (20 mg/kg) (n = 9 mice per group). Pooled data from in vivo experiments (n = 9 mice per group) showing mean fluorescence intensities (MFIs) of PD-L1 on intratumoral macrophages (*K*) percentage of TNFα-producing TAMs relative to intratumoral TAMs (*L*) and percentage of IL-10-producing TAMs from control, AB680-, palbociclib-, and AB680 plus palbociclib-administered tumor-bearing mice (n = 6 per group) (*M*). Data have been presented as mean ± standard error of the mean. $^{++}P < .01$ AB680-treated vs vehicle-treated group; $^{\#\#}P < .01$ palbociclib-treated vs vehicle-treated group; $^{*}P < .05$, $^{**}P < .01$, and $^{***}P < .001$ AB680 plus palbociclib-treated vs vehicle-treated group (Student *t* test).

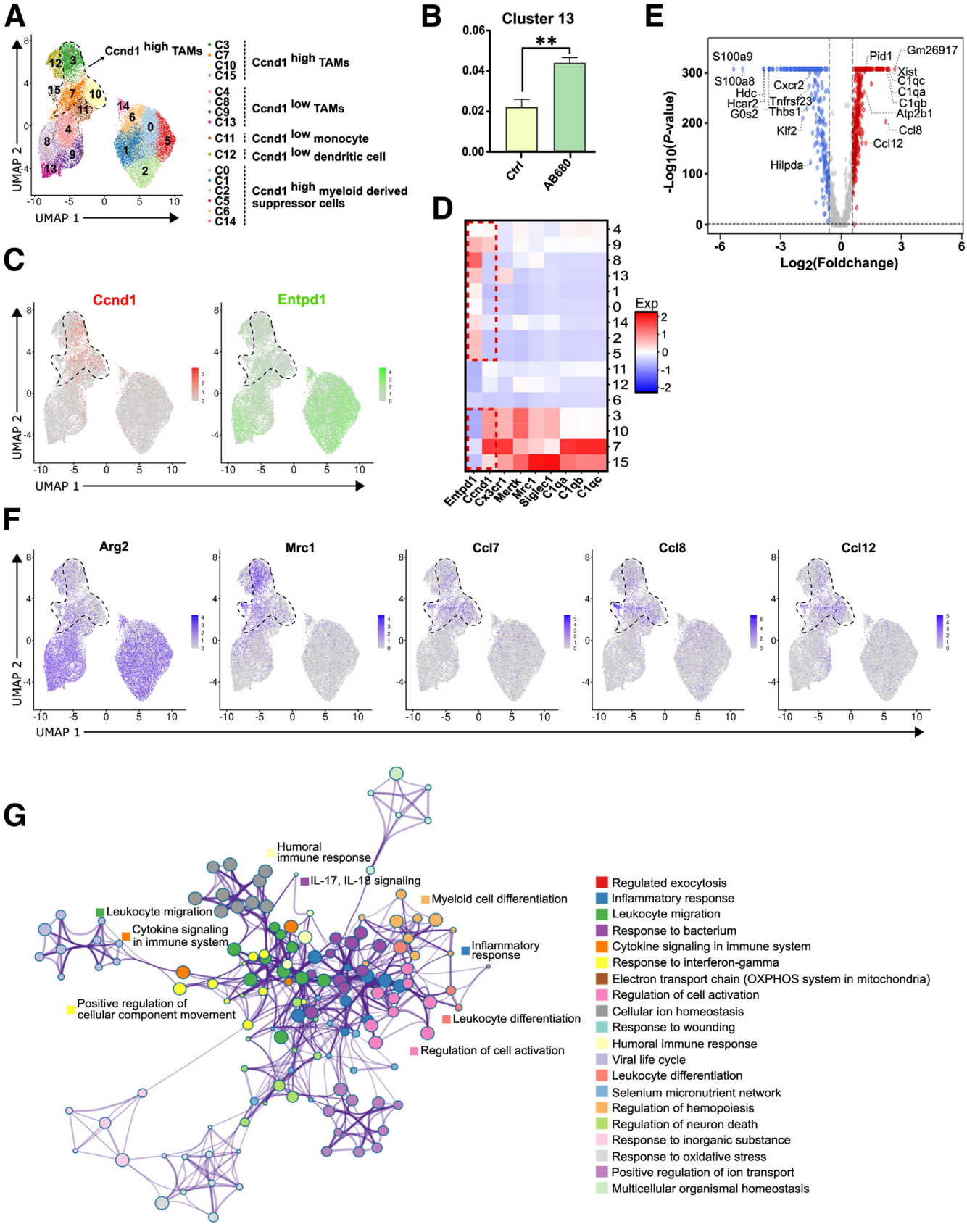
A
Ccnd1 high TAMs
C3
C7
C10
C15
Ccnd1 high TAMs
C4
C8
C9
C13
Ccnd1 low TAMs
C11
Ccnd1 low monocyte
C12
Ccnd1 low dendritic cell
C0
C1
C2
C5
C6
C14
Ccnd1 high myeloid derived suppressor cells
UMAP 1
UMAP 2
B
Cluster 13
**
Ctrl
AB680
C
Ccnd1
Entpd1
D
Exp
Entpd1
Ccnd1
Cx3cr1
Mertk
Mrc1
Siglec1
C1qa
C1qb
C1qc
E
S100a9
S100a8
Hdc
Hcar2
G0s2
Cxcr2
Tnfrsf23
Thbs1
Klf2
Hilpda
Pid1
Gm26917
Xist
C1qc
C1qa
C1qb
Atp2b1
Ccl8
Ccl12
-Log10(P-value)
Log2(Foldchange)
F
Arg2
Mrc1
Ccl7
Ccl8
Ccl12
G
Humoral immune response
IL-17, IL-18 signaling
Myeloid cell differentiation
Leukocyte migration
Cytokine signaling in immune system
Inflammatory response
Positive regulation of cellular component movement
Leukocyte differentiation
Regulation of cell activation
Regulated exocytosis
Inflammatory response
Leukocyte migration
Response to bacterium
Cytokine signaling in immune system
Response to interferon-gamma
Electron transport chain (OXPHOS system in mitochondria)
Regulation of cell activation
Cellular ion homeostasis
Response to wounding
Humoral immune response
Viral life cycle
Leukocyte differentiation
Selenium micronutrient network
Regulation of hemopoiesis
Regulation of neuron death
Response to inorganic substance
Response to oxidative stress
Positive regulation of ion transport
Multicellular organismal homeostasis

with CRC.[35,36] Previous clinical studies have reported the possibilities of increased CD73 expression in gastric, liver, pancreatic, and colorectal cancers, as biomarkers for poor prognosis and malignancy.[15,20] In this study, we demonstrated for the first time that extracellular adenosine can directly upregulate PD-L1 expression in human macrophages. The immunosuppressive adenosine was potentially produced by the ectoenzymes CD39 and CD73, and accordingly, the CD73 inhibitor AB680 significantly reduced PD-L1 levels in both human macrophages and TAMs obtained from mouse models of CRC. More importantly, the additive effect of AB680 and the CDK4/6 inhibitor palbociclib on tumor growth was observed in the animal models (Figure 7, *G* and *J*), whereas only AB680 could control PD-L1 levels in TAMs (Figure 7, *I* and *K*). This demonstrates that novel drug candidates targeting the adenosine signaling pathway, specifically CD73 inhibitors, could benefit patients who are resistant to anti-PD-1/PD-L1 immunotherapy, by means of a combination strategy.[23,37] In line with this, TCGA analysis confirmed a trend for a lower overall survival rate in patients with CRC who had high expression of *NT5E* compared with those with a low expression of *NT5E*, thereby suggesting that CD73 could play a critical role in tumor progression.[25]

In a large proportion of cases, anti-cancer therapies, such as pemetrexed, doxorubicin, and Palbociclib, trigger increased expression of PD-L1, which is a major obstacle for cancer treatment.[30,31] Notably, CDK4/6 inhibitor monotherapy, which interferes with the G1/S phase checkpoint during the cell cycle, has failed to control tumor growth owing to the accumulation of PD-L1 protein after treatment.[38,39] Thus, the promising effects of CD73 inhibitors might breathe new life for those old drugs and provide potent therapeutic strategies. Given that the therapeutic effects of PD-1/PD-L1 immunotherapy have not been conclusively demonstrated in patients with CRC, our observations should support clinical trials of new combinational therapies for CRC. Because palbociclib is undergoing clinical trials for metastatic CRC in combination with cetuximab (clinical trial number: NCT03446157), this study could provide helpful information for future clinical trials on refractory CRC.

Cyclin D1 plays a central role in tumorigenesis in cancer cells and is an important regulator of the cell cycle.[40] In general, cyclin D1 is known for its role in the nucleus, in cell cycle regulation, but it is also located in the cytoplasmic membrane and plays important roles in the regulation of specific miRNAs, tumor invasion, and metastasis. It has also been reported that cyclin D1 is involved in post-translational regulation of PD-L1 via CDK4-related SPOP regulation.[26] In this study, we discovered a similar mechanism could occur in human macrophages or TAMs, upon extracellular adenosine exposure in the TME, which is a novel finding. We found that adenosine repressed *CCND1* mRNA expression in macrophages, resulting in increased PD-L1 expression (Figure 2). It seems that the adenosine receptor-mediated intracellular cAMP increase may play a role in the downregulation of cyclin D1 (Figure 7, *C*), as previously reported.[41-43] Furthermore, we showed that *Ccnd1*^{high} myeloid cells were *Entpd1*-negative or -low, as compared with *Ccnd1*^{low} myeloid cells, which were also functionally distinguished (Figure 9). Taken together, cyclin D1 may be one of the major orchestrators that trigger the differentiation of pro-tumorigenic TAMs. Our findings suggest a novel immune checkpoint regulatory mechanism of extracellular adenosine signaling, which might be related to the cell cycle of macrophages.

We showed that both CUL3 and CUL4B interact with PD-L1, which is important for PD-L1 regulation after adenosine treatment of human macrophages. MLN4924, an NEDD8 inhibitor, induced PD-L1 accumulation, suggesting that cullin-RING ligases could indeed be involved in PD-L1 regulation in macrophages. Notably, CUL3 has been found to be important for PD-L1 ubiquitination and proteasome degradation, downstream of CCND1 and CDK4.[26] Therefore, we hypothesized that a similar mechanism of action occurs in macrophages and, importantly, showed that SPOP reduction could upregulate PD-L1 (Figure 6, *L*–*M*). Interestingly, CUL4B has been reported to play a crucial role in the proliferation and function of myeloid-derived suppressor cells, which is in support of our finding.[44,45] Thus, it is important to identify an appropriate adapter protein for CUL4B in human macrophages and investigate the exact mechanisms of CUL4B-mediated PD-L1 regulation in macrophages in the future. Overall, our results demonstrated a critical PD-L1-regulatory role of extracellular adenosine at the post-translational level.

Taken together, this study highlights the benefits of use of extracellular adenosine signaling inhibitors for reducing PD-L1 expression on TAMs, thereby providing novel and effective strategies for future clinical trials of refractory CRCs. Thus, the association between TAMs and the extracellular adenosine signaling-mediated strong tumorigenic effects reported in this study will hopefully aid the future development of TAM-targeting cancer immunotherapies.

Figure 9. (***See previous page***). **Network analysis of DEGs from *Ccnd1*^{high} and *Ccnd1*^{low} intra-tumoral myeloid cells.** (*A*) Distinct transcriptional profiles of *Ccnd1*^{high} and *Ccnd1*^{low} intra-tumoral myeloid cells obtained from the CT26 tumor cell-bearing mouse model. Uniform manifold approximation and projection (UMAP) plot for myeloid cell subclusters. (*B*) Proportion of myeloid cluster 13 between the control and AB680-treated tumors. (*C*) UMAP plot for the expression of *Ccnd1 and Entpd1* in myeloid cells. (*D*) Heat map representing cluster-specific gene expressions. (*E*) Volcano blot for *Ccnd1*^{low} intra-tumoral myeloid cells, compared to *Ccnd1*^{high} intra-tumoral myeloid cells. (*F*) UMAP plot for the expression of inflammatory response- and leukocyte migration-related genes. (*G*) Comparative scRNA-seq analysis of *Ccnd1*^{low} intratumoral myeloid cells, as compared with *Ccnd1*^{high} intratumoral myeloid cells. In the functional network, each node represents a GO biological pathway, and the edges indicate the relationships among biological pathways, based on kappa values.

Materials and Methods

Generation and Treatment of Monocyte-derived Macrophages and 3D Culture of Macrophages

Primary monocytes were isolated from human PB as previously described.[46] PB from healthy individuals was obtained from the Korean Red Cross Blood Center (Wonju, Korea), and the study protocol was approved by the institutional review board of the Red Cross, in accordance with the principles of the Declaration of Helsinki. To induce differentiation into macrophages, isolated human monocytes were cultured in the presence of recombinant human macrophage colony-stimulating factor (M-CSF, 20 ng/mL; PeproTech, Rocky Hill, NJ) in RPMI-1640 medium (Life Technologies, Carlsbad, CA) containing 10% fetal bovine serum (FBS; Life Technologies), L-glutamine (2 mM), and 1% penicillin-streptomycin (Life Technologies) at 37 °C, in an incubator with 5% CO_2. The medium was replenished every 3 days. On day 6, the generated macrophages were treated with various ATP concentrations (5, 10, 20, 50, 100, 200, and 400 μg/mL; CAS no: 34369-07-8; Sigma-Aldrich, St. Louis, MO), adenosine (5, 10, 20, 50, 100, 200, and 400 μg/mL; CAS no: 58-61-7; Sigma-Aldrich) and AB680 (2 μg/mL; CAS no. 2105904-82-1; MedChemExpress, Monmouth Junction, NJ) or CPI-444 (2 μg/mL; CAS no. 1202402-40-1; Selleckchem, Houston, TX) for 48 hours. For PD-L1 accumulation, MG-132 (CAS. No. 1211877-36-9) and MLN4924 (CAS. No. 951950-33-7) were purchased from Sigma-Aldrich.

For 3D culture of macrophages, differentiated macrophages from primary monocytes were washed with Dulbecco's phosphate-buffered saline (Gibco, Thermo Fisher Scientific,Waltham, MA), dissociated with Accutase, and seeded into 12-well plates (5×10^4 cells/well) coated with a 1.5% agarose gel (Invitrogen, Carlsbad, CA) in α-MEM supplemented with 10% heat-inactivated FBS and 1% penicillin-streptomycin. Treatment with ATP or adenosine (Sigma-Aldrich) in a 3D environment was initiated 48 hours after seeding and continued for 3 days.

Antibodies and Flow Cytometry

For the fluorescence-activated cell sorting analysis, cells were stained with APC,-anti human CD163 (clone: GHI/61), PD-anti human CTLA4 (clone: L3D10), Alexa 647-anti human IDO1 (clone: 2E2/IDO1), PE-anti human DR4 (clone: DJR1), FITC-anti human CD47 (clone: REA220, FITC-anti human MICA&B (clone: 6D4), PE-anti human PD-L1 (clone: MIH2), PD-anti human CD69 (clone: FNM50), FITC-anti human CD2 (clone: RPA-2.10), FITC-anti human CD20 (clone: 2H7), APC-anti mouse F4/80 (clone: BM8), Brilliant Violet 421™-anti mouse CD11b (clone: M1/70), Brilliant Violet 570™-anti mouse CD45 (clone: 104), PE-anti-human CD45 (clone: HI30), monoclonal antibodies (Biolegend; San Diego, CA, USA), FITC-anti-human CD40 (clone: REA733), PE-anti human CD80 (clone: 2D10), PE/vio770-anti human CD206 (clone: DCN228), PE-anti human CD62E (clone: REA280), PE-anti human CD192 (clone: REA264), APC-anti human I-CAM (clone: REA266), APC-anti human HLA-DR, DP, DQ (clone: REA332), APC-anti human CCL2 (clone: REA485), APC-anti human CD14 (clone: HI30), Vioblue-anti human CD31 (clone: TUK4), FTIC-anti-human CD86 (clone: FM95), PE-anti human CD73 (clone: AD2), PE-anti mouse PD-L1 (clone: 60533), PE-anti mouse CD39, and PE-anti human CD39 (clone: REA739) monoclonal antibodies (Miltenyi Biotec; Bergisch Gladbach, Germany), and PE/CF594-anti human CD3 (clone: UCHT1), PE-anti human CD44 (clone: G44-26), PE-anti human CD183 (clone: 150503), and PD-1 (clone: REA739) monoclonal antibodies (BD Biosciences; San Jose, CA, USA) following the manufacturer's protocol. Cells were incubated on ice for 20 minutes, washed with chilled annexin V binding buffer, and analyzed. Data were collected using a MACSQuant Analyzer VYB (Miltenyi Biotec).

Lentiviral Vector Constructs

A full-length human *CD274* (encoding PD-L1) cDNA clone (SC115168; pCMV6-XL4-PDL1) was purchased from OriGene Technologies (Rockville, MD). FLAG-tagged PD-L1 (NM_014143) was constructed using p3xFLAG-CMV10 and amplified for cloning into a lentiviral vector, pLVX-EF1α-IRES-puro. cDNA of SPOP (NM_003563) was purchased from the Korea Human Gene Bank (Daejeon, Korea). The *SPOP* gene was fused with an HA- or Myc-tag and combined with pcDNA3.1 or pLVX-EF1α-IRES-puro, respectively. Plasmids encoding HA-tagged ubiquitin (AB089617) and Myc-tagged Cullin-3 (CUL3; NM_003590) were purchased from Addgene (#18712 and #19893, respectively) and assembled with pLVX-EF1α-IRES-puro. Myc-tagged *CCND1* (NM_053056) was synthesized by Macrogen (Seoul, Korea) and conjugated with pLVX-EF1α-IRES-puro. shRNAs against *CUL3*, *CUL4B*, *SPOP*, and *CCND1* were purchased from Macrogen and inserted into a pLKO.1-puro vector to generate lentiviruses, as previously described.

Quantitative Reverse Transcription Polymerase Chain Reaction (qRT-PCR)

Total RNA was isolated from human macrophages using the QIAzol RNA lysis reagent (Qiagen, Valencia, CA, USA). cDNA was synthesized from RNA using a PrimeScript RT reagent kit (Takara Bio, Tokyo, Japan) according to the manufacturer's instructions. qPCR was performed using Power SYBR Green PCR master mix (Applied Biosystems, Foster City, CA) and a QuantStudio 3 real-time PCR system (Applied Biosystems) following manufacturer's instruction. Glyceraldehyde 3-phosphate dehydrogenase (*GAPDH*) served as a housekeeping gene for normalization. Experiments were performed in triplicate. The primers used are listed here. *CCND1*-1-F: 5'-AGCTGTGCATCTACACCGAC-3', *CCND1*-1-R: 5'-GAAATCGTGCGGGGTCATTG-3', *CCND1*-2-F: 5'-CAACCTCCTCAACGACCGG-3', *CCND1*-2-R: 5'-ACTTCTGTTCCTCGCAGACC-3', *CCND2*-1-F: 5'-CGACTCCGAAGTCCCATCTG-3', *CCND2*-1-R: GGCTTGATGGAGTTGTCGGT-3', *CCND2*-2-F: 5'-TTGAAGTGGAACCTGGCAGC-3', *CCND2*-2-R: AGCATGCTTGCGGATCAGAG-3', *CCND3*-1-F: CGAGTATGGAGCTGCTGTGT-3', *CCND3*-1-R: 5'-CACGCACTGGAAGTAGGAGG-3', *CCND3*-2-F: 5'-GTATGGAGCTGCTGTGTTGC-3', *CCND3*-2-R: 5'-

GCACGCACTGGAAGTAGGAG-3', *PD-L1*-1-F: 5'-GCTATGGTGGTGCCGACTACAA-3', *PD-L1*-1-R: 5'-GGTGGTGGTCTTACCACTCAGGA-3'

Western Blotting

Human macrophages were filtered through a cell strainer (70 μm; Falcon) and pelleted for lysis. Protein samples were boiled for 10 minutes, separated by electrophoresis in 12% sodium dodecyl sulfate polyacrylamide gels, and transferred onto nitrocellulose membrane (Amersham Biosciences, Buckinghamshire, UK). The membrane were blocked with 5% skim milk and probed with a rabbit anti-PD-L1 antibody (1:1,000; Cell Signaling Technology, Danvers, MA), rabbit anti-CDK4 antibody (1:500; Cell Signaling Technology), rabbit anti-SPOP antibody (1:1,000; Proteintech, Tokyo, Japan), anti-cyclin D1 antibody (1:1,000, Cell Signaling Technology), or mouse anti-β-actin antibody (1:5,000, Cell Signaling Technology) at 4 °C overnight. The membranes were then incubated with horseradish peroxidase-conjugated anti-mouse or anti-rabbit IgG (Sigma-Aldrich) for 1 hour. Protein bands were visualized using enhanced chemiluminescence reagents (Amersham Biosciences).

Immunoprecipitation (IP)

An IP lysis buffer (150 mM NaCl, 25 mM Tris-HCl, 10% glycerol, and 1 mM EDTA) containing a protease inhibitor cocktail (Roche, Basel, Switzerland) was used for cell lysis. After centrifugation at 12,000 $\times$ g for 20 minutes at 4 °C, equal amounts of protein were incubated overnight at 4 °C with anti-HA, anti-Myc (Cell Signaling Technology), anti-FLAG (Sigma-Aldrich) primary antibodies, and a rabbit polyclonal IgG antibody (Cell Signaling Technology) as a negative control. Subsequently, the samples were incubated with protein A/G Sepharose beads (GE Healthcare, Waukesha, WI) at 4 °C for 2 hours. The immunocomplexes were washed 5 times with lysis buffer, boiled, and analyzed using Western blot, with 1:500 dilutions of anti-HA, anti-Myc, and anti-FLAG primary antibodies.

Immunohistochemical (IHC) Staining

Tissue microarrays for normal and cancerous human colon tissues (sample ID: BC05118d) were purchased from Biomax (Rockville, MD). The tissue microarray samples were dried for 20 minutes at 60 °C, deparaffinized with xylene, and rehydrated. Antigens were retrieved by heating the sections at 95 °C in 0.01 M sodium citrate buffer, pH 6.0. Endogenous peroxidase activity was blocked using 3% hydrogen peroxide. The samples were stained with antibodies against cyclin D1 (1:100, MA5-16356; Thermo Fisher Scientific) and CD163 (1:100, MA5-11458; Thermo Fisher Scientific). Incubation with a biotin-conjugated secondary antibody and visualization were performed using the VECTASTAIN Elite ABC-HRP kit (Vector Laboratories, Burlingame, CA), followed by counterstaining with hematoxylin. The processed slides were analyzed under a light microscope (IX53; Olympus, Tokyo, Japan) using the CellSens Dimension program. Cyclin D1 immunostaining intensity in macrophage-enriched areas of colon tissues was analyzed using ImageJ software (National Institutes of Health, Rockville, MD).

Enzyme-linked Immunosorbent Assay (ELISA)

Human PBMC derived macrophage supernatants were collected, centrifuged at 1500 rpm for 10 minutes at 4 °C and stored in −80 °C until further use. These samples were used to measure the secretory levels of TNF-α and IL-10 by ELISA using a LEGNEND MAX kit (Biorad Technologies, UK) according to the manufacturer's instructions (Biolegend, San Diego, CA).

Intracellular cAMP Analysis

Macrophages were differentiated in α-MEM medium supplemented with 10% (v/v) heat-inactivated FBS, 1% (v/v) penicillin-streptomycin, and 20 ng/mL human M-CSF at 37 °C in 5% CO_2 for 7 days. After then, differentiated macrophages were incubated in α-MEM medium without FBS at 37 °C incubator for 2 hours and stimulated with ATP and/or AB680 in the presence of 200 uM 3-Isobutyl-1-methylxanthine (IBMX, Sigma-Aldrich) for 1 hour. Intracellular cAMP was measured using commercially available cAMP-GloTM assay kit (Promega, Madison, WI) according to the manufacturer's protocol.

Liquid Chromatography–Tandem Mass Spectrometry (LC-MS/MS)

Human macrophages were transduced with the PD-L1-FLAG-expressing lentivirus and cultured in the presence or absence of 200 μM adenosine. In-gel digestion of immunoprecipitated proteins was performed for peptide analysis. The gels were sliced into seven fractions according to their molecular weight and destained with a solution containing 10 mM ammonium bicarbonate and 50% acetonitrile. Tryptic in-gel digestion of proteins was performed in 50 mM ammonium bicarbonate at 37 °C for 12 to 16 hours. Tryptic peptides were analyzed using LC-MS/MS. All MS and MS/MS spectra were acquired using an LTQ-Velos ESI ion trap mass spectrometer (Thermo Fisher Scientific) in the data-dependent mode. For protein identification, MS/MS spectra were searched for using MASCOT (version 2.4; Matrix Science, UK) in the mouse protein database downloaded from UniProt (www.uniprot.org). Each sample was subjected to MS/MS analysis in triplicate. For protein quantification, the mol% value was calculated from the emPAI value using the MASCOT program.[47,48] DEPs were defined as abs (log ratio) $\geq$0.2. Gene set enrichment tests for GO were performed using Enrichr.[49] A protein-protein interaction network was constructed using STRING v11.[50]

Illumina RNA-seq

Total RNA was isolated from macrophages, and an RNA-seq library was generated using the TruSeq Stranded Total RNA LT sample prep kit (Illumina, San Diego, CA), according to the manufacturer's instructions. Briefly, mRNA was

separated from the total RNA using oligo (dT) beads and chemically fragmented. After double-stranded cDNA synthesis from the fragmented mRNA, end repair, adenylation of the 3′ end, and sequencing adapter ligation were performed, followed by DNA purification with magnetic beads and PCR amplification. Finally, the amplified library was purified, quantified, and used for template preparation. The NovaSeq 6000 platform (Illumina) was used to generate 101-bp paired-end sequencing reads, which were mapped to the reference genome sequence of *Mus musculus* (UCSC mm10) using HISAT2 version 2.1.0.[51] The mapped reads were assembled using StringTie version 1.3.4d,[52] merged for each condition (untreated and adenosine treated groups), and quantified using read counts and fragments per kilobase of transcript per million mapped reads. Finally, DEGs were identified using the criteria of a fold change of 2 and a nbinormWaldTest raw *P*-value of $< .05$. The expression volume of each gene was estimated using transcript assembly.

Clustering Analysis

We reprocessed clustering scRNA-seq data downloaded from the Sequence Read Archive under accession number SUB8983993, to determine the transcriptional profiles of *Ccnd1*^{low} and *Ccnd1*^{high} myeloaid cells in a tumor-bearing mouse model.[25] We used *FindVariableFeatures* in the Seurat package to identify highly variable genes and then performed principal component analysis with the top 2000 variable genes. Clusters were partitioned using *FindClusters* in the Seurat package, and the cells were projected into a 2-dimensional space with uniform manifold approximation and projection (UMAP). The DEGs in each cluster were identified using *FindMarkers* in the Seurat package. We also used the SingleR[53] method.

The Cancer Genome Atlas (TCGA) Data Analysis

NT5E and *CCND1* mRNA expression and patient survival data, grouped by colon cancer, were derived from TCGA data portal (http://cancergenome.nih.gov/). The data in TCGA included RNA-seq expression, whole-genome sequencing, and clinical phenotype data for colon cancer. Genomic and clinical data for colon cancer samples were downloaded from TCGA data portal (https://www.cbioportal.org/). RNA-seq data were analyzed using reads per kilobase of transcripts per million mapped reads. All analyses were performed using R package. The Kaplan-Meier method was used to plot the survival curves. The survival records of patients who were alive at the final follow-up were censored.

Gene Set Enrichment Analysis

Representative DEG-related biological pathways were analyzed using the Metascape web portal,[54] including GO.[55] Pairwise similarities between any 2 enriched biological pathways were computed based on a kappa test score.[56] The most significant pathways (*P*-value 0.01) were clustered based on pairwise similarities. The hypergeometric test and Benjamini-Hochberg *P*-value correction algorithm were used to identify all biological pathway terms that contained a statistically greater number of genes in common with an input list than that expected by chance.

Animal Model

Male BALB/c mice (6–8 weeks old) were purchased from Orientbio, Inc. (Seongnam, Gyeonggi-do, Korea) and housed in a pathogen-free animal facility. All animal experiments were approved by the Institutional Animal Care and Use Committee of the Korea Research Institute of Chemical Technology in accordance with the Guide for the Care and Use of Laboratory Animals published by the United States National Institutes of Health. A tumor-bearing model was established by subcutaneous injection of 1×10^6 CT26 cells (ATCC CRL-2638™; American Type Culture Collection, Manassas, VA) into the right flanks of mice. Four days after inoculation, the mice were randomly divided into control, AB680-treated, and Palbociclib-treated groups ($n = 9$ mice per group). The CD73 inhibitor AB680 (20 mg/kg) (MedChemExpress) and Palbociclib (20 mg/kg) (MedChemExpress) were administered intraperitoneally from day 0 to day 18 after inoculation. Tumors were measured every 2 days using calipers. Tumor volumes were calculated as: volume (mm^3) = ($d^2 \times D$)/2, where d and D represent the shortest and longest tumor diameters, respectively. To analyze macrophages and T cells from tumor tissues, a whole CT26 tumor (~3–4 mm) was harvested from a sacrificed mouse and placed in 10 mL of ice-cold DPBS. The tumor tissue was thoroughly cut and minced with a scalpel into fragments of $\leq$0.5 mm. A cell suspension of the minced tumor was generated using a tumor dissociation kit (Miltenyi Biotec) following the manufacturer's protocol. CD45-positive tumor-infiltrating lymphocytes were analyzed using fluorescence-activated cell sorting.

AOM-DSS Murine Model

All animal experiments were approved by the Institutional Animal Use and Care Committee of the Korea Research Institute of Chemical Technology and performed in accordance with the Guide for the Care and Use of Laboratory Animals published by the United States National Institutes of Health. A colitis-associated cancer model mouse was made by intraperitoneal injection of 10 mg/kg AOM (Sigma-Aldrich, st. Louis, MO) and by oral administration of 2.5% DSS with a molecular weight of 36,000–50,000 (MP Biomedicals, Santa Ana, OH). Five-week-old male C57BL/6J mice (Orientbio, Inc., Seongnam, Gyeonggi-do, Korea) a were acclimatized for the first week. At 6 weeks of age, mice were randomly divided into a control healthy group ($n = 8$), AOM/DSS group ($n = 8$), and AOM/DSS + AB680 or Palbociclib treated group ($n = 8$). Seven days after AOM injection, 2.5% DSS was given in the drinking water over 7 days, followed by 14 days of regular water. Three cycles of DSS treatment were repeated. AB680 (10 mg/kg) (MedChemExpress) and Palbociclib (20 mg/kg) (MedChemExpress) were administered from day

0 to 21 after the end of the third cycle of DSS treatment via the intraperitoneal (i.p.) route. All mice were sacrificed at the end of the experiments (at day 21 after the third cycle of DSS treatment), and the colons were obtained. Each colon was cut open longitudinally, and the normal tissue of the proximal colon, dysplasia tissue of the middle colon, and cancer tissue of the distal colon were distinguished and assessed using a stereoscopic microscope. For flow cytometry analysis, we generated cell suspension of the minced colon tissues using an Intestine Dissociation Kit (Miltehyi Biotec, Bergisch Gladbach, Germany) following the manufacturer's protocol.

Statistical Analysis

All statistical tests were performed using directed pairwise comparisons. Unpaired t tests were performed to analyze differences between two groups. Statistical significance was defined as $P < .05$. Data are presented as the mean ± standard error of the mean. Statistical analyses were performed using the Prism software (GraphPad Software, La Jolla, CA).

References

1. Das S, Ciombor KK, Haraldsdottir S, Goldberg RM. Promising new agents for colorectal cancer. Curr Treat Options Oncol 2018;19:29.
2. Jung G, Benítez-Ribas D, Sánchez A, Balaguer F. Current treatments of metastatic colorectal cancer with immune checkpoint inhibitors-2020 update. J Clin Med 2020;9:3520.
3. Hirano H, Takashima A, Hamaguchi T, Shida D, Kanemitsu Y. Colorectal Cancer Study Group (CCSG) of the Japan Clinical Oncology Group (JCOG). Current status and perspectives of immune checkpoint inhibitors for colorectal cancer. Jpn J Clin Oncol 2021;51:10–19.
4. Jácome AA, Eng C. Role of immune checkpoint inhibitors in the treatment of colorectal cancer: focus on nivolumab. Expert Opin Biol Ther 2019;19:1247–1263.
5. Lee JJ, Chu E. Recent advances in the clinical development of immune checkpoint blockade therapy for mismatch repair proficient (pMMR)/non-MSI-H metastatic colorectal cancer. Clin Colorectal Cancer 2018; 17:258–273.
6. Bray F, Ferlay J, Soerjomataram I, Siegel RL, Torre LA, Jemal A. Global cancer statistics 2018: GLOBOCAN estimates of incidence and mortality worldwide for 36 cancers in 185 countries. CA Cancer J Clin 2018; 68:394–424.
7. Nguyen M, Tipping Smith S, Lam M, Liow E, Davies A, Prenen H, Segelov E. An update on the use of immunotherapy in patients with colorectal cancer. Expert Rev Gastroenterol Hepatol 2021;15:291–304.
8. Scheurlen KM, Billeter AT, O'Brien SJ, Galandiuk S. Metabolic dysfunction and early-onset colorectal cancer - how macrophages build the bridge. Cancer Med 2020; 9:6679–6693.
9. Kasprzak A. The role of tumor microenvironment cells in colorectal cancer (CRC) cachexia. Int J Mol Sci 2021; 22:1565.
10. Mantovani A, Marchesi F, Malesci A, Laghi L, Allavena P. Tumour-associated macrophages as treatment targets in oncology. Nat Rev Clin Oncol 2017;14:399–416.
11. De Palma M, Lewis CE. Macrophage regulation of tumor responses to anticancer therapies. Cancer Cell 2013; 23:277–286.
12. Herbst RS, Soria JC, Kowanetz M, Fine GD, Hamid O, Gordon MS, Sosman JA, McDermott DF, Powderly JD, Gettinger SN, Kohrt HE, Horn L, Lawrence DP, Rost S, Leabman M, Xiao Y, Mokatrin A, Koeppen H, Hegde PS, Mellman I, Chen DS, Hodi FS. Predictive correlates of response to the anti-PD-L1 antibody MPDL3280A in cancer patients. Nature 2014;515:563–567.
13. Montalbán Del Barrio I, Penski C, Schlahsa L, Stein RG, Diessner J, Wöckel A, Dietl J, Lutz MB, Mittelbronn M, Wischhusen J, Häusler SFM. Adenosine-generating ovarian cancer cells attract myeloid cells which differentiate into adenosine-generating tumor associated macrophages - a self-amplifying, CD39- and CD73-dependent mechanism for tumor immune escape. J Immunother Cancer 2016;4:49.
14. Zanin RF, Braganhol E, Bergamin LS, Campesato LF, Filho AZ, Moreira JC, Morrone FB, Sévigny J, Schetinger MR, de Souza Wyse AT, Battastini AM. Differential macrophage activation alters the expression profile of NTPDase and ecto-5′-nucleotidase. PLoS One 2012;7:e31205.
15. Messaoudi N, Cousineau I, Arslanian E, Henault D, Stephen D, Vandenbroucke-Menu F, Dagenais M, Létourneau R, Plasse M, Roy A, Lapointe R, Ysebaert D, Trudel D, Soucy G, Stagg J, Turcotte S. Prognostic value of CD73 expression in resected colorectal cancer liver metastasis. Oncoimmunology 2020;9:1746138.
16. Yang R, Elsaadi S, Misund K, Abdollahi P, Vandsemb EN, Moen SH, Kusnierczyk A, Slupphaug G, Standal T, Waage A, Slørdahl TS, Rø TB, Rustad E, Sundan A, Hay C, Cooper Z, Schuller AG, Woessner R, Borodovsky A, Menu E, Børset M, Sponaas AM. Conversion of ATP to adenosine by CD39 and CD73 in multiple myeloma can be successfully targeted together with adenosine receptor A2A blockade. J Immunother Cancer 2020;8:e000610.
17. Bours MJ, Swennen EL, Di Virgilio F, Cronstein BN, Dagnelie PC. Adenosine 5′-triphosphate and adenosine as endogenous signaling molecules in immunity and inflammation. Pharmacol Ther 2006;112:358–404.
18. Leone RD, Emens LA. Targeting adenosine for cancer immunotherapy. J Immunother Cancer 2018;6:57.
19. Allard D, Allard B, Stagg J. On the mechanism of anti-CD39 immune checkpoint therapy. J Immunother Cancer 2020;8:e000186.
20. Harvey JB, Phan LH, Villarreal OE, Bowser JL. CD73's potential as an immunotherapy target in gastrointestinal cancers. Front Immunol 2020;11:508.
21. Allard B, Longhi MS, Robson SC, Stagg J. The ectonucleotidases CD39 and CD73: novel checkpoint inhibitor targets. Immunol Rev 2017;276:121–144.
22. Bowman CE, da Silva RG, Pham A, Young SW. An exceptionally potent inhibitor of human CD73. Biochemistry 2019;58:3331–3334.

23. Lawson KV, Kalisiak J, Lindsey EA, Newcomb ET, Leleti MR, Debien L, Rosen BR, Miles DH, Sharif EU, Jeffrey JL, Tan JBL, Chen A, Zhao S, Xu G, Fu L, Jin L, Park TW, Berry W, Moschütz S, Scaletti E, Sträter N, Walker NP, Young SW, Walters MJ, Schindler U, Powers JP. Discovery of AB680: a potent and selective inhibitor of CD73. J Med Chem 2020;63:11448–11468.
24. Fong L, Hotson A, Powderly JD, Sznol M, Heist RS, Choueiri TK, George S, Hughes BGM, Hellmann MD, Shepard DR, Rini BI, Kummar S, Weise AM, Riese MJ, Markman B, Emens LA, Mahadevan D, Luke JJ, Laport G, Brody JD, Hernandez-Aya L, Bonomi P, Goldman JW, Berim L, Renouf DJ, Goodwin RA, Munneke B, Ho PY, Hsieh J, McCaffery I, Kwei L, Willingham SB, Miller RA. Adenosine 2A receptor blockade as an immunotherapy for treatment-refractory renal cell cancer. Cancer Discov 2020;10:40–53.
25. Kim M, Min YK, Jang J, Park H, Lee S, Lee CH. Single-cell RNA sequencing reveals distinct cellular factors for response to immunotherapy targeting CD73 and PD-1 in colorectal cancer. J Immunother Cancer 2021;9:e002503.
26. Zhang J, Bu X, Wang H, Zhu Y, Geng Y, Nihira NT, Tan Y, Ci Y, Wu F, Dai X, Guo J, Huang YH, Fan C, Ren S, Sun Y, Freeman GJ, Sicinski P, Wei W. Cyclin D-CDK4 kinase destabilizes PD-L1 via cullin 3-SPOP to control cancer immune surveillance. Nature 2018;553:91–95.
27. Wang L, Zhou X, Zhou T, Ma D, Chen S, Zhi X, Yin L, Shao Z, Ou Z, Zhou P. Ecto-5'-nucleotidase promotes invasion, migration and adhesion of human breast cancer cells. J Cancer Res Clin Oncol 2008;134:365–372.
28. Young A, Ngiow SF, Barkauskas DS, Sult E, Hay C, Blake SJ, Huang Q, Liu J, Takeda K, Teng MWL, Sachsenmeier K, Smyth MJ. Co-inhibition of CD73 and A2AR adenosine signaling improves anti-tumor immune responses. Cancer Cell 2016;30:391–403.
29. Vigano S, Alatzoglou D, Irving M, Ménétrier-Caux C, Caux C, Romero P, Coukos G. Targeting adenosine in cancer immunotherapy to enhance T-cell function. Front Immunol 2019;10:925.
30. Okimoto T, Kotani H, Iida Y, Koyanagi A, Tanino R, Tsubata Y, Isobe T, Harada M. Pemetrexed sensitizes human lung cancer cells to cytotoxic immune cells. Cancer Sci 2020;111:1910–1920.
31. Naba NM, Tolay N, Erman B, Sayi Yazgan A. Doxorubicin inhibits miR-140 expression and upregulates PD-L1 expression in HCT116 cells, opposite to its effects on MDA-MB-231 cells. Turk J Biol 2020;44:15–23.
32. Gschweitl M, Ulbricht A, Barnes CA, Enchev RI, Stoffel-Studer I, Meyer-Schaller N, Huotari J, Yamauchi Y, Greber UF, Helenius A, Peter M. A SPOPL/Cullin-3 ubiquitin ligase complex regulates endocytic trafficking by targeting EPS15 at endosomes. Elife 2016;5:e13841.
33. Gao J, Buckley SM, Cimmino L, Guillamot M, Strikoudis A, Cang Y, Goff SP, Aifantis I. The CUL4-DDB1 ubiquitin ligase complex controls adult and embryonic stem cell differentiation and homeostasis. Elife 2015;4:e07539.
34. Aubry A, Yu T, Bremner R. Preclinical studies reveal MLN4924 is a promising new retinoblastoma therapy. Cell Death Discov 2020;6:2.
35. Liu N, Fang XD, Vadis Q. CD73 as a novel prognostic biomarker for human colorectal cancer. J Surg Oncol 2012;106:918–919; author reply: 920.
36. Wu XR, He XS, Chen YF, Yuan RX, Zeng Y, Lian L, Zou YF, Lan N, Wu XJ, Lan P. High expression of CD73 as a poor prognostic biomarker in human colorectal cancer. J Surg Oncol 2012;106:130–137.
37. Sitkovsky MV. Lessons from the A2A adenosine receptor antagonist-enabled tumor regression and survival in patients with treatment-refractory renal cell cancer. Cancer Discov 2020;10:16–19.
38. Otto T, Sicinski P. Cell cycle proteins as promising targets in cancer therapy. Nat Rev Cancer 2017;17:93–115.
39. Knudsen ES, Witkiewicz AK. The strange case of CDK4/6 inhibitors: mechanisms, resistance, and combination strategies. Trends Cancer 2017;3:39–55.
40. Montalto FI, De Amicis F. Cyclin D1 in cancer: a molecular connection for cell cycle control, adhesion and invasion in tumor and stroma. Cells 2020;9:2648.
41. Haskó G, Linden J, Cronstein B, Pacher P. Adenosine receptors: therapeutic aspects for inflammatory and immune diseases. Nat Rev Drug Discov 2008;7:759–770.
42. Verweij P, Danaietash P, Flamion B, Ménard J, Bellet M. Randomized dose-response study of the new dual endothelin receptor antagonist aprocitentan in hypertension. Hypertension 2020;75:956–965.
43. Smith SA, Newby AC, Bond M. Ending restenosis: inhibition of vascular smooth muscle cell proliferation by cAMP. Cells 2019;8:1447.
44. Qian Y, Yuan J, Hu H, Yang Q, Li J, Zhang S, Jiang B, Shao C, Gong Y. The CUL4B/AKT/β-catenin axis restricts the accumulation of myeloid-derived suppressor cells to prohibit the establishment of a tumor-permissive microenvironment. Cancer Res 2015;75:5070–5083.
45. Hung MH, Jian YR, Tsao CC, Lin SW, Chuang YH. Enhanced LPS-induced peritonitis in mice deficiency of cullin 4B in macrophages. Genes Immun 2014;15:404–412.
46. Bellows CG, Aubin JE, Heersche JN, Antosz ME. Mineralized bone nodules formed in vitro from enzymatically released rat calvaria cell populations. Calcif Tissue Int 1986;38:143–154.
47. Yun SH, Park EC, Lee SY, Lee H, Choi CW, Yi YS, Ro HJ, Lee JC, Jun S, Kim HY, Kim GH, Kim SI. Antibiotic treatment modulates protein components of cytotoxic outer membrane vesicles of multidrug-resistant clinical strain, Acinetobacter baumannii DU202. Clin Proteomics 2018;15:28.
48. Lee SY, Kim GH, Yun SH, Choi CW, Yi YS, Kim J, Chung YH, Park EC, Kim SI. Proteogenomic characterization of monocyclic aromatic hydrocarbon degradation pathways in the aniline-degrading bacterium Burkholderia sp. K24. PLoS One 2016;11:e0154233.

49. Kuleshov MV, Jones MR, Rouillard AD, Fernandez NF, Duan Q, Wang Z, Koplev S, Jenkins SL, Jagodnik KM, Lachmann A, McDermott MG, Monteiro CD, Gundersen GW, Ma'ayan A. Enrichr: a comprehensive gene set enrichment analysis web server 2016 update. Nucleic Acids Res 2016;44:W90–97.
50. Szklarczyk D, Gable AL, Lyon D, Junge A, Wyder S, Huerta-Cepas J, Simonovic M, Doncheva NT, Morris JH, Bork P, Jensen LJ, Mering CV. STRING v11: protein-protein association networks with increased coverage, supporting functional discovery in genome-wide experimental datasets. Nucleic Acids Res 2019; 47:D607–D613.
51. Kim D, Langmead B, Salzberg SL. HISAT: a fast spliced aligner with low memory requirements. Nat Methods 2015;12:357–360.
52. Pertea M, Pertea GM, Antonescu CM, Chang TC, Mendell JT, Salzberg SL. StringTie enables improved reconstruction of a transcriptome from RNA-seq reads. Nat Biotechnol 2015;33:290–295.
53. Aran D, Looney AP, Liu L, Wu E, Fong V, Hsu A, Chak S, Naikawadi RP, Wolters PJ, Abate AR, Butte AJ, Bhattacharya M. Reference-based analysis of lung single-cell sequencing reveals a transitional profibrotic macrophage. Nat Immunol 2019;20:163–172.
54. Zhou Y, Zhou B, Pache L, Chang M, Khodabakhshi AH, Tanaseichuk O, Benner C, Chanda SK. Metascape provides a biologist-oriented resource for the analysis of systems-level datasets. Nat Commun 2019;10:1523.
55. Ashburner M, Ball CA, Blake JA, Botstein D, Butler H, Cherry JM, Davis AP, Dolinski K, Dwight SS, Eppig JT, Harris MA, Hill DP, Issel-Tarver L, Kasarskis A, Lewis S, Matese JC, Richardson JE, Ringwald M, Rubin GM, Sherlock G. Gene ontology: tool for the unification of biology. The Gene Ontology Consortium. Nat Genet 2000;25:25–29.
56. Roberts C. Modelling patterns of agreement for nominal scales. Stat Med 2008;27:810–830.

Received March 22, 2021. Accepted July 8, 2022.

Correspondence

Address correspondence to: Dr Chang Hoon Lee, Therapeutics & Biotechnology Division, Drug Discovery Platform Research Center, Korea Research Institute of Chemical Technology (KRICT), Daejeon, Republic of Korea. e-mail: ch.lee@sc-bio.co.kr; tel: +82-42-860-7414; Dr Daeui Park, Department of Predictive Toxicology, Korea Institute of Toxicology, Daejeon, Korea. e-mail: daeui.park@kitox.re.kr; tel: +82-42-610-8251.

CRediT Authorship Contributions

Ji-Yoon Noh, PhD (Investigation: Equal; Writing – original draft: Supporting)
In Pyo Lee, MS (Investigation: Lead; Methodology: Lead)
Na Rae Han, PhD (Investigation: Equal)
Miok Kim, PhD (Formal analysis: Lead; Investigation: Lead; Methodology: Lead)
Yong Ki Min, PhD (Data curation: Equal; Formal analysis: Supporting)
Sang-Yeop Lee, PhD (Formal analysis: Lead)
Sung Ho Yun, MS (Formal analysis: Equal; Investigation: Equal)
Seung Il Kim, PhD (Formal analysis: Equal)
Tamina Park, MS (Formal analysis: Lead)
Hyunmin Chung, MS (Investigation: Supporting)
Daeui Park, PhD (Formal analysis: Lead; Investigation: Equal)
Chang Hoon Lee, PhD (Conceptualization: Lead; Data curation: Lead; Funding acquisition: Lead; Investigation: Lead; Writing – original draft: Lead; Writing – review & editing: Lead)

Conflicts of interest

The authors disclose no conflicts.

Funding

This work was supported by National research foundation of Korea (NRF) of the the Korean government (grant no. 2021R1C1C1011899), the Korea Institute of Planning and Evaluation for Technology in Food, Agriculture, Forestry (IPET) through the Animal Disease Management Technology Development Program of the Ministry of Agriculture, Food, and Rural Affairs (MAFRA) of the Korean government (grant no. 318070-3), by the Intramural Research Fund (1711159828) of KIT, and by the Intramural Research Fund (SI2231-10) of KRICT from the Korean government.

Availability of data

Proteomics data supporting the findings of this study have been deposited to the ProteomeXchange Consortium via the PRIDE43 partner repository with the dataset identifier PXD024512. RNAseq data supporting the findings of this study have been deposited to the BioProject ID: PRJNA708316. RNA-seq data that support the finding study have been in deposited to the NCBI SRA database (https://www.ncbi.nlm.nih.gov/sra) with the dataset identifier PRJNA708316. In PRJNA708316, there are 6 RNA-seq files for macrophage as control condition and adenosine-treated macrophage. All authors had access to the study data and reviewed and approved the final manuscript.